Permian Sequence stratigraphy in east-central Iran: Microplate records of Peri-Tethyan and Peri-Gondwanan events

Sakineh Arefifard[1] and Peter E. Isaacson[2]
[1]*Geology Department, Faculty of Sciences, Lorestan University, Iran*
[2]*Department of Geological Sciences, University of Idaho, Moscow, Idaho, USA 83844-3022*
email: sarefifard@gmail.com

ABSTRACT: Permian rocks in east-central Iran (Posht-e-Badam and Tabas blocks) belong to well-defined sequences in juxtaposed Early and Late Permian biogeographic provinces. The Lower Permian Khan Formation in the Kalmard area (Within the Posht-e- Badam block) is composed of cyclic sequences of thick compositionally and texturally mature sandstones and thin carbonates. The sequences reflect several nearshore microfacies, which constitute three major paleoenvironmental associations: tidal flat, lagoon, and shoal (open marine microfacies are missing or very rare). The carbonate rocks of the Lower through Upper Permian Jamal Formation in the Shotori and Shirgesht areas (within the Tabas block) are comprised of four microfacies indicative of tidal flat, lagoon, foreshore and open marine paleoenvironments. The Jamal Formation was deposited on a homoclinal carbonate ramp, which deepens to the north (Bagh-e-Vang section) and thins in southern locations (near the Jamal Formation type section). The Khan Formation succession is composed of second- and third-order cyclically siliciclastic and carbonate sequences. The Jamal carbonate is composed of second- and third-order shallowing-upward sequences. Both local tectonic activity and global eustacy may have controlled the cyclicity of the Khan and Jamal formations.

INTRODUCTION

Permian strata of the Jamal and Khan formations in east-central Iran contain highly diverse fossil faunas. The Jamal Formation occurs in the Shotori area (east and southeast of Tabas) and the Shirgesht area (north of Tabas), within the Tabas structural block (text-fig. 1). Most descriptions of the formation were made in the 1960s by Stocklin et al. (1965) and Ruttner et al. (1968). The age of the Jamal Formation, which is composed mostly of carbonates (text-fig. 2), has been suggested to be Early to Late Permian in age (Stocklin et al. 1965; Ruttner et al. 1968; Kahler 1974, 1977; Jenny-Deshusses 1983; Partoazar 1992; Leven and Taheri 2003; Leven and Vaziri Moghaddam 2004).

In the Kalmard area, within the Posht-e Badam block, the Khan Formation (Aghanabati 1977) is represented by cyclic sequences of siliciclastics and carbonates. Recent biostratigraphic studies on this formation are based on fusulinids, and they provide a late Sakmarian to early Artinskian age (Davydov and Arefifard 2007). The time of deposition of the Khan Formation corresponds to a major unconformity between the Carboniferous Sardar and the Permian Jamal formations in the Shirgesht and Ozbak Kuh areas (north of the Tabas) (Davydov and Arefifard 2007). The fusulinid faunas of the Khan Formation show a Peri-Gondwanan affinity compared to the Peri-Tethyan fusulinid faunas of the Jamal Formation. This indicates that there were different paleobiogeographic histories for the central Iranian blocks (text-fig. 1). Although biostratigraphic studies have been carried out for many decades in the Posht-e-Badam and Tabas structural blocks, no microfacies and sequence stratigraphic analyses have been conducted on the Permian sections. The purpose of this contribution is to describe and document facies, depositional environments and sequence stratigraphy of the Jamal and Khan formations.

GEOLOGICAL HISTORY

Central Iran is tectonically complex and has a long geologic history. This area has been named as the central Iran microcontinent (Takin 1972), middle triangle (Nogolsadat 1978), central domain (Stocklin 1977) and central Iran blocks (Alavi 1991) (text-fig. 1).

This terrane is part of the Cimmerian continent (Sengor 1984) that rifted away from north Gondwana at the end of the Paleozoic (Scotese and Langford 1995; Dercourt et al. 1993). One idea is that the Permian–Middle Triassic approach, and successive Late Triassic collision, of some Cimmerian blocks with Laurasia along a north-directed subduction zone closed the Paleotethys Ocean during the Triassic in the so-called Early or Eo-Cimmerian orogeny (Brunet et al. 2009). Another model suggests that Neo-Tethys 1 came into being when the Central Iran Microcontinent split from the northeastern margin of Gondwana during the Late Carboniferous to Early Permian. During the Late Triassic a new spreading ridge, Neo-Tethys 2, was created and separated the Shahrekord–Dehsard Terrane from the Afro–Arabian Plate (Arfania and Shahriari 2009). According to Wendt et al. (2002, 2005), the Southern Alborz as well as the Yazd, Tabas and Lut blocks, belonged to the stable northern margin of Gondwana during the Paleozoic. They also noted that much of northern and central Iran was subject to uplift, switching many depositional systems from marine to continental in the Pennsylvanian. They stated that a new marine cycle commenced in the Early Permian, and large parts of the northern Gondwana margin were subducted during the collision

with Eurasian plates in the Upper Triassic closure of Paleotethys.

Alavi (1991) divided central Iran into four tectonic blocks including the Lut (LB), Tabas (TB), Posht-e-Badam (PBB) and Yazd blocks (YB), based on strike-slip dextral faults (Nayband, Kuhbanan, Kalmard and Posht-e-Badam) (text-fig. 1). The Shotori and Shirgesht areas are situated in the Tabas block and separated from the Posht-e-Badam block by the north-south trending Kalmard and Kuhbanan faults (text-fig. 2). The Kalmard area is located in the Posht-e-Badam block and bounded by the Kalmard and Naeini faults. The region was formed as a mobile zone throughout the Paleozoic. Berberian and King (1981) described intense Paleozoic subsidence that occurred within the Tabas block. It was previously thought that this subsidence was confined to the Shirgesht and Ozbak-Kuh areas in the extreme north of Tabas (Stocklin 1971), but later it was found that the entire block was subsiding throughout the Paleozoic and Mesozoic (Berberian and King 1981). The Tabas block has been considered to be a failed rift basin throughout Devonian to Late Triassic times, which formed during the Paleotethys, rifting as a result of the Early Ordovician-Silurian continental extension along its bounding Nayband and Kalmard-Kuhbanan fault systems (Lasemi 2001 and 2008).

In east-central Iran, fragmentation of the metamorphic basement followed a late Precambrian orogeny, and the Shotori basin subsided by active Precambrian extensional faults. More than 7000 m of Paleozoic epicontinental marine sediments were deposited within the Tabas block. Conversely, the Paleozoic deposits in the Kalmard area (within the Posht-e-Badam block) are only 950 m thick (Berberian 1983). The differences in thickness and sedimentary facies indicate that the Kalmard and Tabas faults were active and continued to be the principal cause of differential basin subsidence during Paleozoic time in these two areas.

LITHOSTRATIGRAPHY AND BIOSTRATIGRAPHY

For this study eight Permian stratigraphic sections in the Kalmard, Shotori, Shirgesht areas were measured, collected and described (text-fig. 2). All the sections are well exposed, although some of them are slightly deformed by Mesozoic and more recent tectonics.

Khan Formation - late Sakmarian-early Artinskian

Lithostratigraphy

In the Kalmard area, sections of the Khan Formation include the following: the type section of the formation at Bakhshi, which is located in the southeast of Kalmard Karevansaray, approximately 92km west of Tabas; the Madbeiki section, 12km west of the Bakhshi section; the Gachal section, nearly 100km southwest of Tabas; the Rahdar section, 65km west of Tabas; and the Halvan section, 80km northwest of Tabas; see text-figure 2.

We collected 546 samples for microfacies analyses and paleontological studies from these sections. The Khan Formation averages 500 m thick and is bounded by disconformities with the Lower Carboniferous Gachal limestone below and the Lower Triassic vermiculitic limestone within the Sorkh Shale above. Fluvial channels immediately above the lower Gachal Formation document the disconformity between the Gachal and Khan formations. At the disconformity between the Khan Formation and the Sorkh Shale, there is a bauxite horizon in the uppermost portion of the Khan Formation.

The Khan Formation consists of cyclic siliciclastic and carbonate sequences (second- and third-order depositional sequences). Each cycle begins with gravel to cobble conglomerate and very coarse sandstone. The grain size of the siliciclastic components decreases upward, and also grades into sandy limestones. The middle and upper parts of each cycle consist mostly of shallow water thick to medium bedded packstone-grainstone, interbedded with mudstone and wackestone. Also, dolomite and dolomitic limestone in some cycles replaces the limestone. The carbonates are followed by red sandstones and shales. Aghanabati (1977) considered the siliciclastic deposits in the lower and upper parts of each cycle to be indicative of transgressive and regressive phases, respectively.

Biostratigraphy

Based on biostratigraphic data from the Khan Formation, Aghanabati (1977) originally assigned it to an Early to a Late Permian age. This age determination was mainly based on long-ranging smaller foraminifers and brachiopods in the formation. Some fusulinids, such as *Triticites primaries isfarensis* Bensh and *Pseudofusulina alpine antique* (Schellwien), were reported by Kahler (1977) from the Kalmard area, without precise information on sample locations. He assigned these fusulinid species to the Pennsylvanian. Haftlang (1998) and Gorgij (2002) studied the lower part of the Khan Formation and concluded that it belonged to the Mississippian. They further stated that it did not contain Permian faunas. Work on fusulinids of the Khan Formation by Davydov and Arefifard (2007) gave a Sakmarian through an early Artinskian age (text-fig. 3). They found Peri-Gondwana fossil assemblages in the Khan Formation, with *Eoparafusulina, Perigondwania* and *Neodutkevichia*, indicative of a late Sakmarian to an early Artinskian age. These fusulinids exhibit affinities to their counterparts in central Pamir, South Afghanistan, east Hindukush and South Tibet. It should be noted that these fusulinids have only been found in limestone of the second cycle of the Khan Formation (Aghanabati's Member B). No index fusulinid taxon has been recorded in the upper part of this formation. Small foraminifers suggest a biostratigraphic age that is no younger than the Early Permian.

Jamal Formation - Artinskian-early Wuchiapingian

The Jamal Formation was studied at three stratigraphic sections in the Shotori and Shirgest areas. In the Shotori area, we used one section of this formation, located 5km east of its type section (text-fig. 2). The lower Jamal Formation has a sharp contact with the Sardar Formation sandstones; its upper boundary is conformable with the Sorkh Formation, although it is faulted in the Shotori area.

Lithostratigraphy

In the Shotori area, the lithologic change between the Sardar and Jamal formations is very conspicuous. Basal beds of the Jamal Formation are sandy limestones with abundant fragmented invertebrate shells. Aghanabati (2004) considered the uppermost siliciclastic rocks of the Sardar Formation as a transgressive sequence in the Jamal Formation. The lower part of this formation consists of grey medium to thick bedded brachiopod and bryozoan bearing wackestone-packstone that is followed by a cream to grey medium to thick bedded

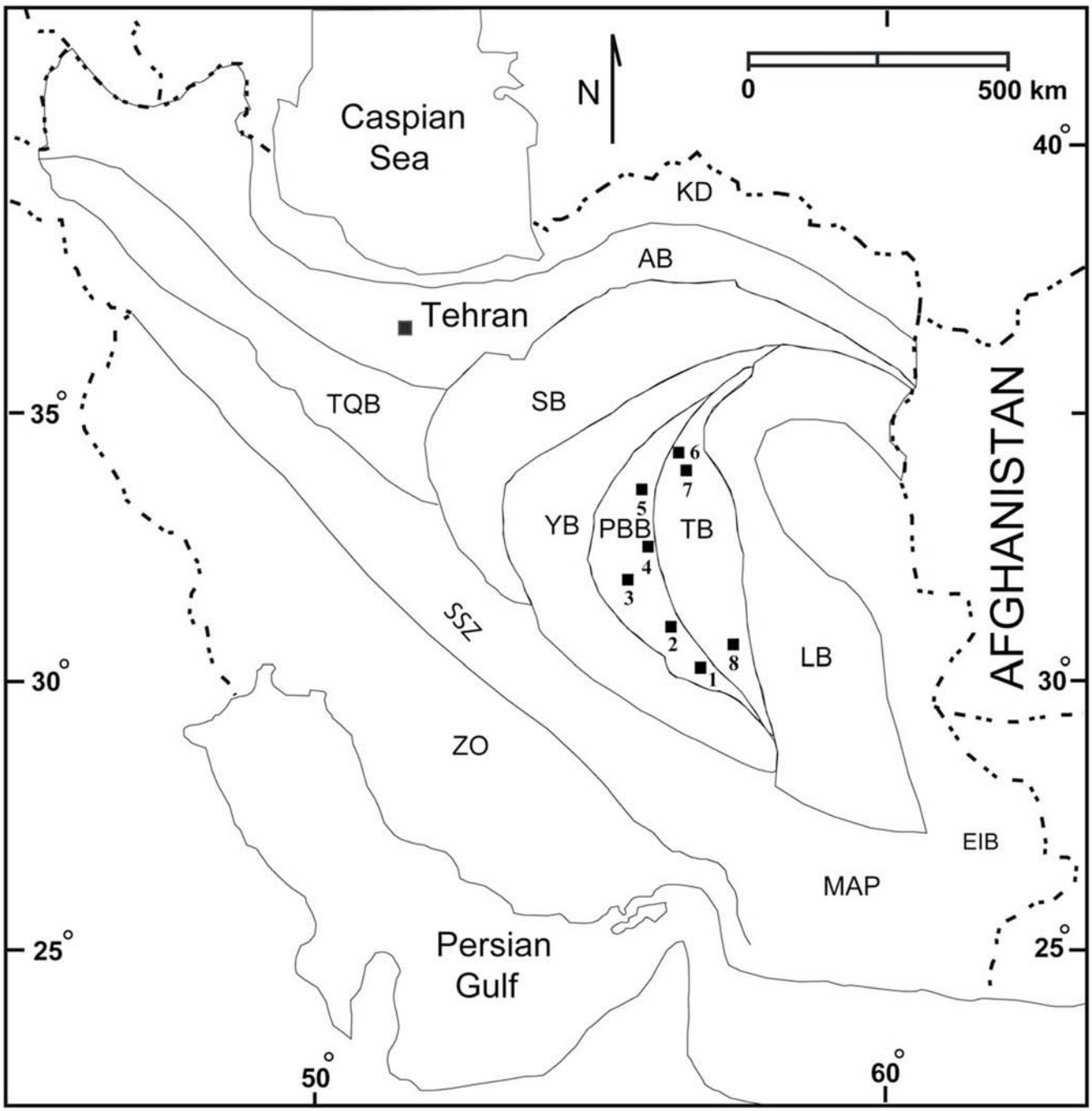

LT=Lut Block
TB=Tabas Block
PBB=Posht-e-Badam Block
YB=Yazad Block
SB=Sabzevar Block
EIB=East Iran Block

AB=Alborz Belt
MAP=Makran accretionary Prism
TQB=Tabriz-Qom Block
ZO=Zagros Orogen
KD=Kopeh Dagh
SSZ= Sanandaj-Sirjan Zone

1 Gachal Section
2 Bakhshi Section
3 Madbeiki Section
4 Rahdar Section
5 Halvan Section
6 Shesh Angosht Section
7 Bagh-e-Vang Section
8 Jamal Section

TEXT-FIGURE 1
Generalised tectonic map of Iran (after Alavi 1991). The central Iran micro-plate is divided into four blocks. The Kalmard area is located within the Posht-e-Badam Block (PBB) whereas the Shotori and Shirgesht areas are in the Tabas Block (TB).

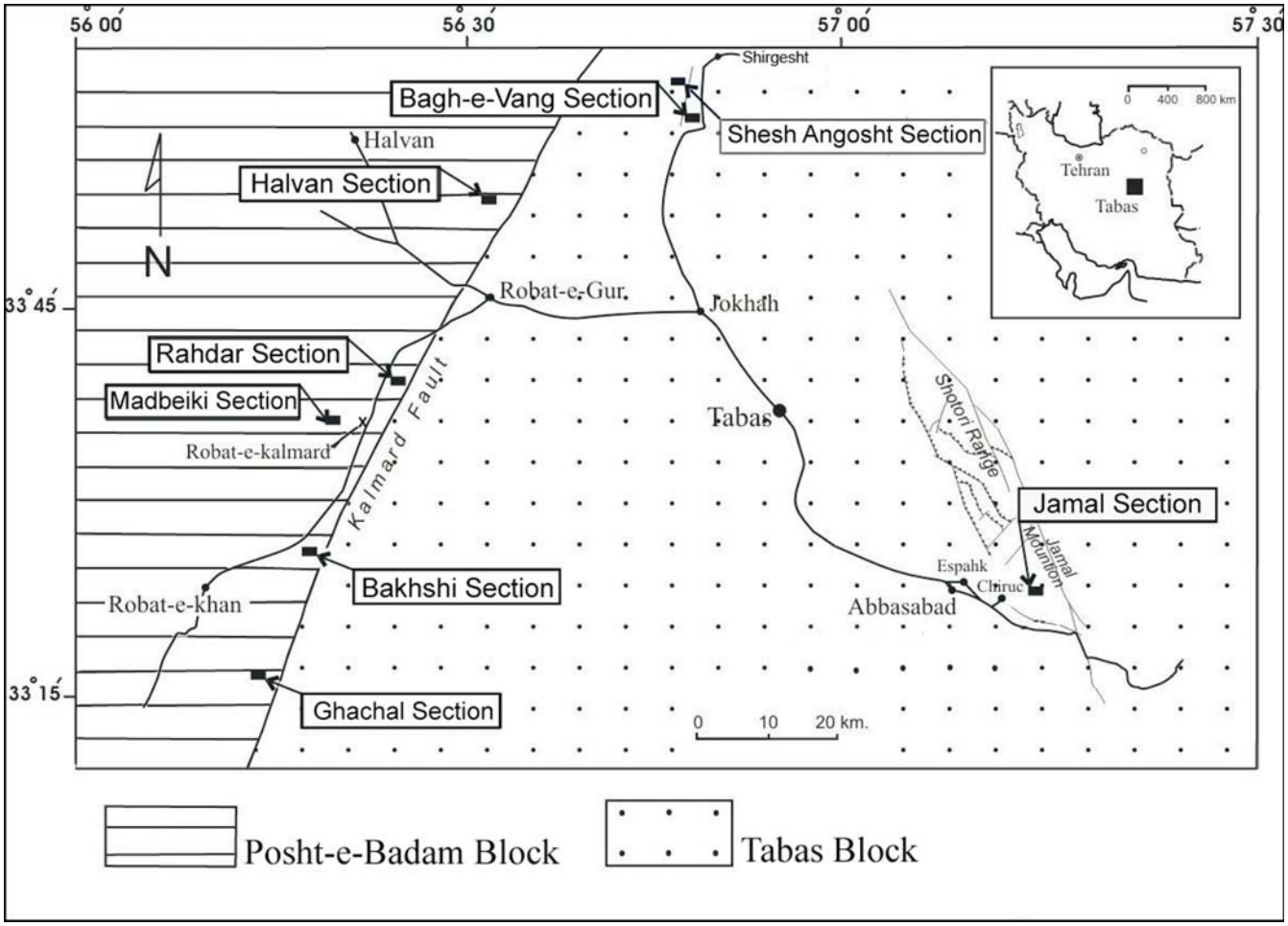

TEXT-FIGURE 2
Index map showing location of the stratigraphic sections. 1 - Gachal, 2 - Bakhshi (type section of the Khan Formation), 3 - Madbeiki, 4 - Rahdar, 5 - Halvan, 6 - Shesh Angosht, 7 - Bagh-e-Vang, 8 - Jamal

grainstone-packstone interbedded with wackestone, micritic limestone and dolomitic limestone. The upper part of the Jamal Formation is dominated by a recrystallized limestone.

In the Shirgesht area, we chose two sections of the Jamal Formation: the Bagh-e-Vang section exposed nearly 50km north of Tabas (text-fig. 2), and the Shesh Angosht section about 4km east of the Bagh-e-Vang section. In both sections the Jamal Formation unconformably overlies Carboniferous red to brown, thin bedded fine sandstones of the Sardar Formation. The upper boundary of the Jamal Formation is conformable with the Lower Triassic Sorkh Shale.

The lower Jamal Formation at the Bagh-e-Vang section consists of carbonate conglomerate or very coarse fusulinid-bearing grainstone. The conglomerate includes pebbles of silty limestone and micritic limestone that is followed by black medium bedded fusulinid grainstone with interbedded shales. Partoazar (1992), and Leven and Vaziri Moghaddam (2004) named this part of the Jamal Formation as the Bagh-e-Vang Member. Based on Stocklin's (1971) interpretation, the limestones in the uppermost portion of the Sardar Formation occur only in northern Tabas, where the Zalado section is exposed in the Ozbakuh area. Further to the south of the Shirgesht area, this part of the Sardar Formation includes a shaly and a sandy facies. These siliciclastic sediments at the top of the Sardar Formation have no biota to date them.

Laterally, the carbonate deposits toward the south were replaced by shaly-sandy sedimentary deposits, and there was a non-depositional phase with erosion before the Jamal Formation sedimentation (Leven and Vaziri Moghaddam 2004). In some outcrops in the Shotori area there is a coal-bearing bed at the top of the Sardar Formation. We suggest that there was a period of subaerial exposure after deposition of the Sardar Formation.

At the Bagh-e-Vang section, the middle Jamal Formation begins with a black, massive and coarse fusulinid-bearing grainstone, and also a local conglomerate bed with a matrix of very coarse grainstone including angular clasts. The remainder of the middle Jamal Formation consists mainly of dark to grey medium to thick bedded cherty micritic limestone with rare medium bedded wackestone-packstone that includes smaller foraminifers and possible radiolaria. Frequency of the wackestone-packstone beds increases upwards. Eventually, they are replaced by a cream to white massive biostromal lime-

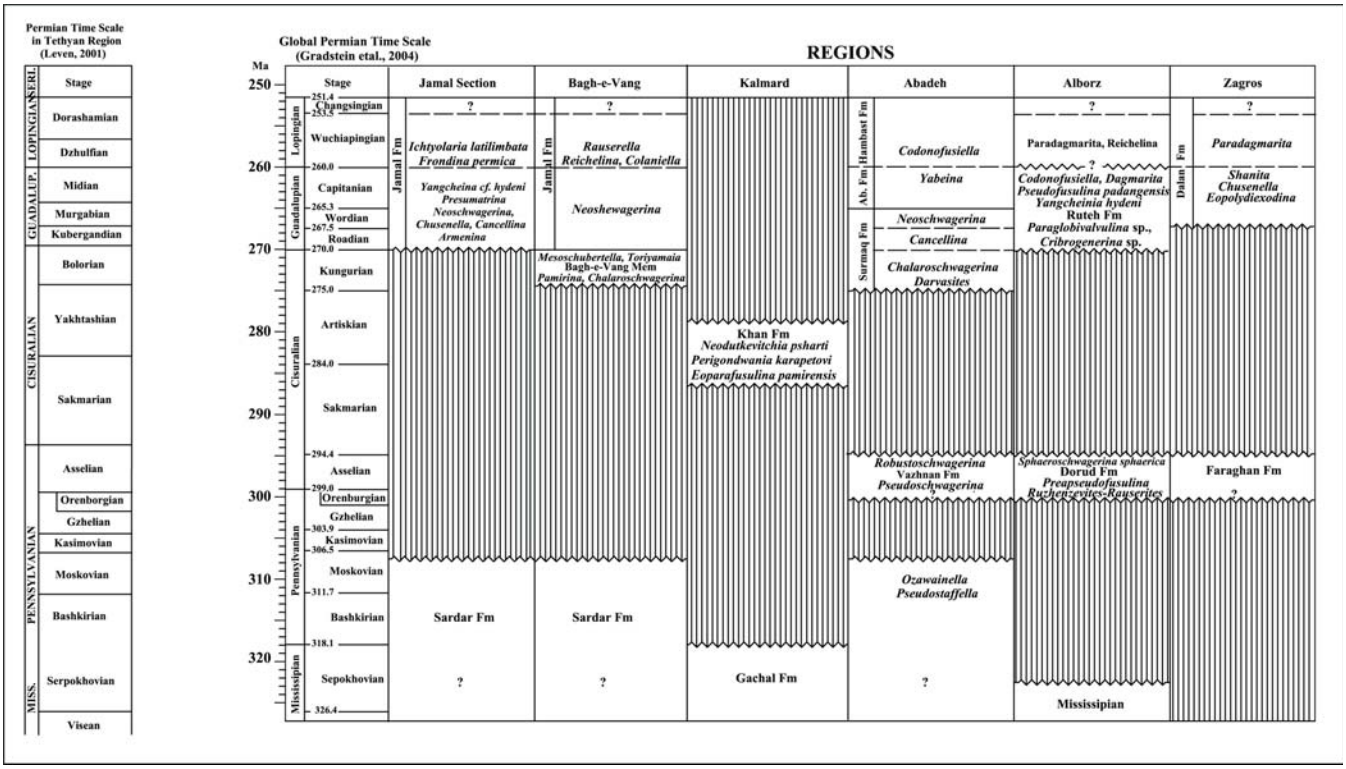

TEXT-FIGURE 3
Correlation chart and references for the Carboniferous-Permian sections in central, east-central, northern and south-west Iran. Bagh-e-Vang and Jamal - Arefifard (2006), Leven and Vaziri Moghaddam (2004); Kalmard - Davydov and Arefifard (2007); Alborz - Gaetani t al. (2009); Abadeh - Baghbani (1993,1997); Zagros –Johnson (1981), Ghavidel-Syooki (1984), Baghbani (1988), Sharland et al. (2001), Insalaco et al. (2006).

stone. Next, the Jamal Formation has smaller foraminifer-bearing wackestone-packstones with cherts. The topmost beds consist of an oolitic limestone and rare beds of dolomite and micritic limestones. The Jamal Formation is overlain by the yellow platy micritic limestone of the Lower Triassic Sorkh shale formation. Although the lithologic features of the Permian strata in the Bagh-e-Vang section differ from those in the Shotori area, a mid ramp setting is suggested for its depositional environment.

At the Shesh Angosht section, the lithology and the thickness of the Jamal Formation differ with its age-equivalent sediments at the Bagh-e-Vang section. The Bagh-e-Vang Member is absent here and the main part of the Jamal Formation is composed of a dark grey massive to medium bedded wackestone-packstone and rare beds of grainstone. We suggest that the marine sedimentary setting was slightly deeper than at the Bagh-e-Vang section, and it may have depositional intervals of starved sedimentation.

Biostratigraphy

Stocklin et al. (1965) described the type section of the Jamal Formation as very poorly fossiliferous, with poorly preserved crinoids, bryozoans (fenestellids), gastropods, brachiopods (productids and spiriferids) from the basal limestone of the formation. Coral-bearing limestone in the middle Jamal Formation have been assigned to the Middle Permian by Bozorgnia (1973), who proposed that its age spanned from the Artinskian (late Early Permian) to the Dzhulfian (early Late Permian), based on the foraminifers. Previous biostratigraphic data (Jenny-Deshusses 1983) suggested a Kubergandian (Roadian) to a Dorashamian (Changsingian) age for the Jamal Formation in the Shotori area. Arefifard (2006) noted that Kubergandian (Roadian) through early Dzhulfian (Wuchiapingian) fusulinid faunas occur there (text-fig. 3).

Early work on the fusulinid-bearing carbonates of the Jamal Formation in the Shirgesht area in the Bagh-e-Vang section (Kahler 1974; Kahler and Kahler 1980) showed that the lower parts of the formation (Bagh-e-Vang Member), with occurrences of some fusulinids (*Pseudofusulina kraffti* (Schellwien and Dyhrenfurth), *Misselina* sp. and *Chalaroschwagerina globosaeformis* (Leven)), are Kungurian (late Early Permian) in age. A preliminary determination of conodonts, cephalopods and corals from this part of the Jamal Formation confirmed this age (Ruttner et al. 1968). Partoazar (1992), working with smaller foraminifers and a fusulinid fauna in the Jamal Formation at the Bagh-e-Vang section, proposed an Asselian through Changsingian age.

In detailed fusulinid studies of the lower part of the Jamal Formation at Bagh-e-Vang, Leven and Vaziri Moghaddam (2004) identified three fusulinid assemblage biozones in the Bagh-e-Vang Member, including the *Pamirina-Mesoschubertella* (Kungurian age), *Paraleeina-Chalaroschwagerina-Misselina* (Kungurian age) and *Misselina-Armenina* (which mark the beginning of the Roadian). Arefifard (2006) assigned an Artinskian-Kungurian age to the lower part of the Jamal Forma-

tion. Only smaller foraminifers and rare fusulinids *(Rauserella, Richelina*) in the middle and upper parts of the Jamal Formation were found at this section. A Roadian to an early Wuchiapingian biostratigraphic age was suggested for this part the Jamal Formation. Fusulinids, such as *Afghanella, Sumatrina* and *Neoschwagerina,* along with other foraminifers in the middle and upper parts of the Jamal Formation in the Bagh-e-Vang section, indicate a Roadian through Wuchiapingian age (Leven and Vaziri Moghaddam 2004). Biostratigraphy of the Khan and Jamal formations, as well as other Permian deposits in Iran are presented in a correlation chart (text-fig.3).

MICROFACIES DESCRIPTION AND INTERPRETATION

A petrographic analysis of the Jamal and Khan formations shows that the several microfacies groups can be arranged into four paleoenvironmental belts. These include the tidal flat sediments (facies A), the lagoon sediments (facies B), the shoal sediments (facies C) and the open marine sediments (facies D).

Jamal Formation Facies

Tidal flat/beach sediments (facies A)

The tidal flat/beach sedimentary deposits are composed of two facies, including a mudstone and a sandy bioclastic grainstone.

A-1- Mudstone

This facies consists of a dark gray, thin- to medium-bedded, planar, unfossiliferous to very sparsely fossiliferous mudstone. Very fine-grained skeletal material, much less than 10% of the lithology, is present. The skeletal grains consist of crinoid stems, brachiopods, foraminifers, and ostracodes. In some cases, aggrading neomorphism causes micrite to be partially altered to microsparite or sparite (text-fig. 4A)

A-2- Sandy Bioclastic Grainstone

The sandy bioclastic grainstone consists of medium-bedded, light gray, partially fossiliferous beds. The fauna includes brachiopods and bivalves. Also, echinoderms form 25 to 30% of the components. Fine- to medium-grained, poorly sorted, angular to subrounded, monocrystalline quartz is also present (approximately 15%). The allochems are cemented by a blocky and drusy sparite (text-fig. 4B).

Interpretation

The lime mudstone with rare skeletal grains indicates a stressed marine environment with a high salinity. Birdseye structures suggest the deposition was in the supratidal to upper intertidal zone (Shinn 1983). The open cavities may be the result of wetting and drying of carbonate mud in a supratidal setting (Shinn 1986). Given the presence of the sand-sized quartz minerals and the lack of micrite, it appears that the sandy bioclastic grainstone was formed in a high energy environment in tidal channels (Shinn 1983).

Lagoon sediments (facies B)

The lagoon sediments are characterized by a bioclastic packstone grainstone/peloid packstone, an intraclast grainstone/ bioclastic wackestone and a peloid bioclastic grainstone.

B-1- Bioclastic packstone-grainstone

This facies consists of gray, medium thickness beds and contains relatively abundant and diverse fauna dominated by echinoderms, brachiopods, green algae, staffellids, smaller foraminifers, gastropods and ostracodes. The bioclast composition is variable, and it thereby includes the following lithologies within this facies: a dasyclad algae staffellid packstone and grainstone; a dacyclad bioclastic packstone-grainstone; and a foraminifer bioclastic packstone-grainstone. There are peloids present in lesser amounts in all lithologies (<3%). The skeletal grains have commonly micritized boundaries that show evidence of boring by endolithic algae (Flügel 2004).

B-2- Peloid packstone

This lithology consists of light gray medium beds of poorly to moderately sorted, angular to subrounded peloids. A minor constituent is smaller foraminifers (3 to 4%). This facies occurs in the lower part of the Jamal Formation (type section) (text-fig. 4C)

TEXT-FIGURE 4

A-B, Photographs of the tidal flat facies of the Jamal Formation.

A Mudstone, note the presence of quartz silt grains.

B Sandy bioclastic grainstone, showing abraded crinoid stems (c) and silt-sized quartz.

C-E, Photomicrographs of the lagoonal facies of the Jamal Formation.

C Peloid packstone with low presence of silt-sized quartz, angular to sub-rounded, poorly sorted peloid are the most common.

D Intraclast grainstone.

E Bioclastic wackestone showing a crinoid stem fragment (c) overlapping a smaller foraminifer shell (f).

F-H, Photomicrographs of the shoal facies of the Jamal Formation.

F Ooid grainstone showing oomolds.

G Bioclast packstone/grainstone showing crinoid stems fragments (c) with syntaxial cement and fenestrate bryozoa fronds (f).

H Intraclast oncoid grainstone showing an algal encrustment around a bioclastic nucleus (o). Scale bar is 0.1mm.

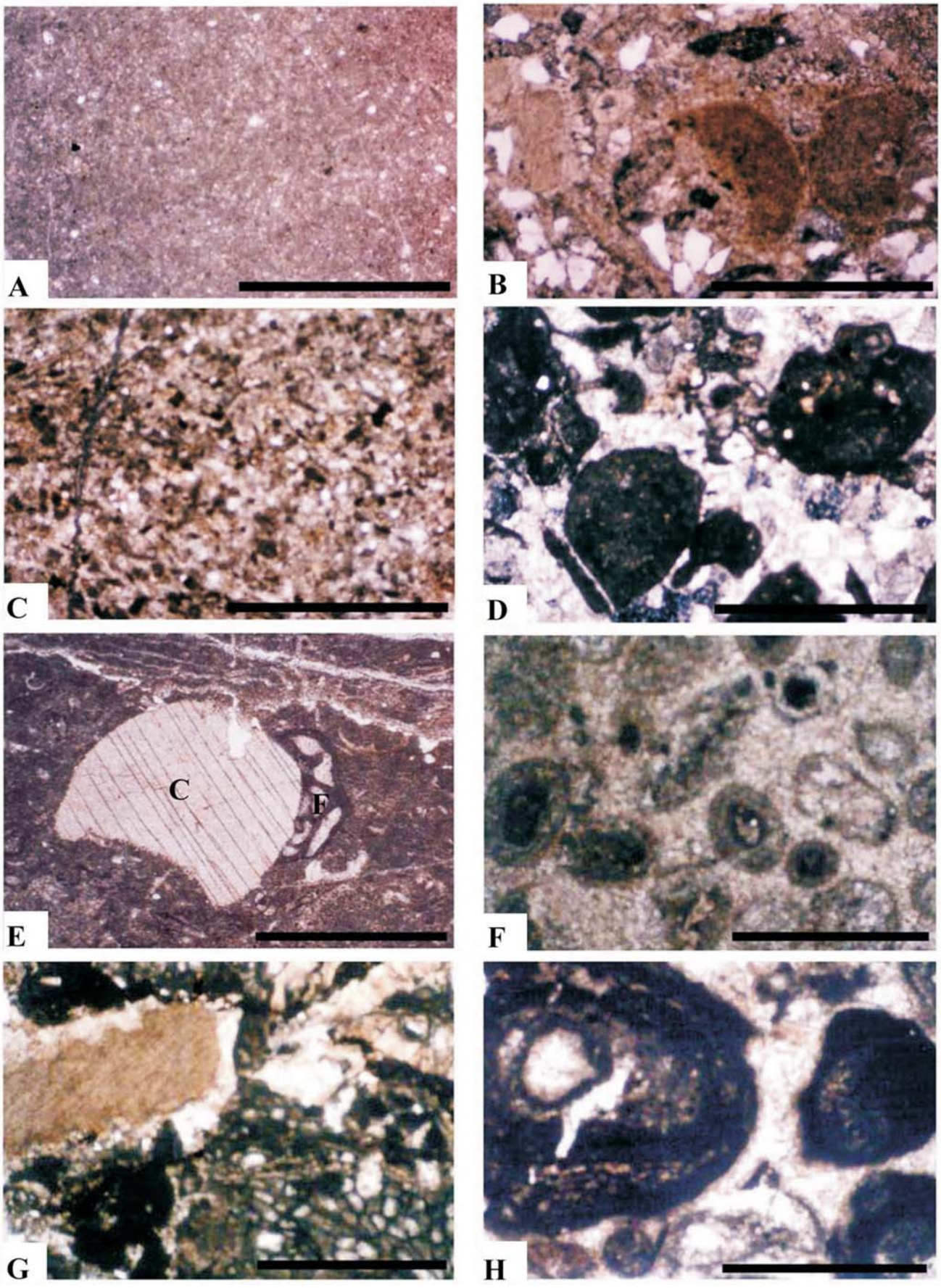
A
B
C
D
C
F
E
F
G
H

B-3- Intraclast grainstone

This facies consists of dark gray, medium to thick beds of angular to subrounded intraclasts (35%). These allochems are surrounded by isopachous cement. The minor allochems are skeletal grains, including staffelids and smaller foraminifers (3 to 4%). The facies grades upward into an intraclast bioclast grainstone. In this latter facies, major allochems are stafellids, dasyclad algae, echinoderms, and brachiopods that form 30% of this facies with 15% micritized-edge intraclasts; less than 5% ooids are present. All the allochems are cemented by sparite. The dasyclad algae and the staffellids are intact (text-fig. 4D).

B-4- Bioclastic wackestone

The bioclastic wackestone is composed of a thin- to medium-bedded dark to light gray, fossiliferous wackestone and a minor peloid bioclastic wackestone with poorly sorted peloids. The skeletal grains include bivalves, brachiopods, smaller foraminifers, echinoderms and ostracodes that form 15% of the bioclastic wackestone. There is quartz, which is a minor allochem (less than 4 to 5 % presence). This facies was observed most frequently in the middle part of the Jamal Formation (Bagh-e-Vang Section) (text-fig. 4E).

B-5- Peloid bioclastic grainstone

This facies consists of gray, medium to thick beds of an oncoid bioclast grainstone, and a fusulinid bioclastic grainstone. The skeletal debris forms 30% of this facies and consists of echinoderms, brachiopods, dasyclad algae and smaller foraminifers. The echinoderm fragments have non-micritized borders. The minor allochems are intraclasts (3%) and ooids (2 to 3%). All the allochems are cemented by drusy, syntaxial and blocky sparites. This microfacies was observed in the middle through the upper parts of the Jamal Formation (at its type section).

Interpretation

The lagoon facies has a relatively abundant fauna. It includes landward, central and leeward shoal sub-environments. The bioclastic packstone-grainstone was deposited in leeward shoal sub-environments with an abundance of dasyclad algae, a lack of normal marine biota, and increased skeletal fragments of restricted fauna. Dasyclad algae are restricted to marine bays and lagoons (Flügel 1982, 2004). The peloid packstone with poorly sorted and angular peloids indicates a shallow intertidal coastal area. They occur preferentially in low-energy zones (Flügel 1982). The occurrence of lime mud indicates a calm environment less affected by waves (Longman 1981). The intraclast grainstone without micritic mud and abundant intraclasts shows a high energy environment and deposition in a leeward shoal setting. The angular intraclasts are produced by the mechanical erosion of lithified beachrocks within the intertidal and the supratidal zones (Flügel 1982, 2004). The bioclastic wackestone suggests a protected shelf region. The micritic background and the low diversity of skeletal grains imply deposition under low energy, quiet water and very restricted conditions. The peloid oncoid bioclast grainstone with close packing was deposited in the upper part of a lagoon toward the shoal, based on its vertical association with a shoal facies. Similar grainstones are forming at margins of oolitic shoals and lower margins of tidal flats in the South Persian Gulf and Shark Bay in Australia.

Shoal sediments (facies C)

The shoal sedimentary deposits are composed of an ooid grainstone/ooid intraclast grainstone, a bioclastic packstone grainstone, and an intraclast oncoid grainstone.

C-1- Ooid grainstone

This facies consists of thick-bedded, fine to coarse-grained ooid grainstone. The well- sorted ooids form 60% of this facies with less than 5% non-coated skeletal debris present. The skeletal debris consists of brachiopods and echinoderms. The ooid grainstone represents shallowing-upward upper ramp shoals (Read 1985). This facies occurs in the upper parts of the Jamal Formation (Bagh-e-Vang Section). Several ooids were exposed to dissolution, and they have lost their original structure and produced oomolds (text-fig. 4F).

C-2- Ooid intraclast grainstone

This facies forms thick-bedded, light to gray beds composed of moderately sorted ooids (25%) and intraclasts (20%) that are

---

TEXT-FIGURE 5

A Photographs of the open marine facies of the Jamal Formation's calcisphere and/or radiolaria wackestone/packstone.

B-F, Photomicrographs of the tidal flat facies of the Khan Formation.

B Mudstone with slit-sized quartz.

C Sandy bioclastic grainstone displaying bioclastic debris with micritized edges and quartz sand grains.

D Sandy intraclast grainstone.

E Sandy ooid grainstone showing the well-sorted ooids with preserved concentric laminae. The ooid nuclei consist of peloid material and sand-sized quartz. Note also the presence of quartz sand grains.

F Quartz sandstone illustrating the well-sorted, angular to sub-angular sand-sized, monocrystalline quartz.

G-H, Photomicrographs of the dolomite facies of the Khan Formation.

G Dolomicrite

H Dolomicrosparite. Scale bar is 0.1.

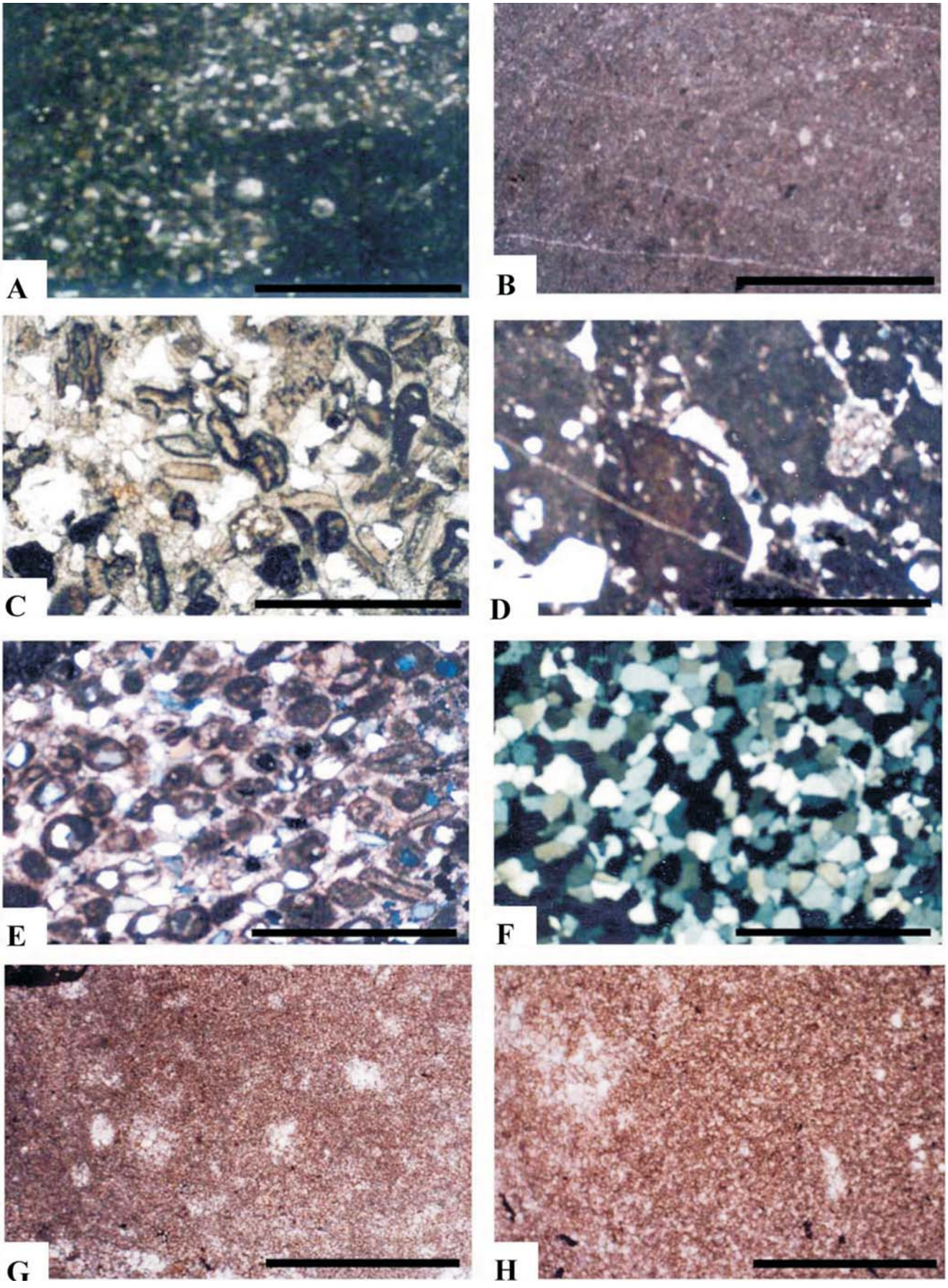
A
B
C
D
E
F
G
H

surrounded by a sparite cement. The bioclasts such as smaller foraminifers, algae and echinoderms are present as less than 5% of the components.

C-3- Bioclastic packstone-grainstone

This facies consists of grayish brown to dark gray, medium- to thick-bedded, fossiliferous beds. The skeletal fragments include brachiopods, echinoderms and unbroken fenestrate bryozoa fronds. Allochems have close packing, producing dissolution-compaction structures such as stylolites. The echinoderm grains show micritized edges. This facies occurs in the middle through upper parts of the Jamal Formation (type section) (text-fig. 4G).

C-4- Intraclast oncoid grainstone

This facies consists of thick-bedded, dark gray beds that include oncoids (20 to 25%) and intraclasts (10 to 15%) as major allochems. The skeletal debris consists of smaller foraminifers, echinoderms and brachiopods that are not parallel-aligned to bedding and are in minor amounts (5%; text-fig. 4H).

Interpretation

The ooid grainstone with tangential structures in this facies indicates a high energy environment that has been subjected to constant wave agitation and produced a well sorted grainstone (Flügel 1982, 2004; Tucker and Wright 1990). The ooid intraclast grainstone implies deposition in the highest energy portion of a seaward shoal within the surf zone. This facies was created in coarsening-upward sedimentary cycles (Reading 1996). The presence of grain-supported and mud-free (or lesser amounts of mud) textures in the bioclastic packstone grainstone indicate that wave and current activity occurred in a high energy depositional environment; i.e., bioclastic shoals developed in a seaward shoal environment. The coarse and whole grains of the intraclast oncoid grainstone suggest that this facies was a leeward shoal.

Open marine sediments (facies D)

The open marine sedimentary deposits include a bioclastic wackestone packstone and a possible radiolaria and/or calcisphere wackestone packstone.

D-1- Bioclastic wackestone-packstone

The bioclast wackestone packstone is composed of thin-bedded, light to dark gray fossiliferous, and bioturbated beds. The skeletal grains include echinoderms, smaller foraminifers and brachiopods that are with a micritic mud matrix.

D-2- Calcisphere and/or radiolaria wackestone-packstone

The calcisphere and/or radiolaria wackestone-packstone consists of a gray medium- to thick-bedded limestone with cherty lenses and nodules along bedding planes. The calcispheres and/or radiolaria are the main allochems in this facies and form up to 35% of the components. Also, sponge spicules are minor allochems and are mostly calcareous. This facies is observed in the middle through upper parts of the Jamal Formation (Bagh-e-Vang Section) (text-fig. 5A).

Interpretation

The occurrence of thin bedding in a bioclastic wackstone-packstone is characteristic of low rates of sedimentation and a low-energy depositional environment. This facies was deposited in the distal part of a carbonate platform or a shallower part of an open marine environment. The abundant deeper water biota contains possible radiolaria, sponges and calcispheres that create intermittent packstone partings (Cadjenovic et al. 2005). The thin-bedding and the cherty nodules together with the calcisphere and radiolaria wackestone-packstone suggest the deeper part of an open marine shelf environment.

Khan Formation Facies

Tidal flat sediments

The tidal flat sedimentary deposits are composed of a mudstone/sandy bioclastic grainstone, a sandy intraclast grainstone, a sandy bioclastic grainstone, and a quartz sandstone.

A-1- Mudstone

The mudstone facies consists of gray, thin to medium beds. Quartz grains and skeletal fragments are minor components. There are some mudstones that are completely replaced by dolomite. Also, gypsum/anhydrite has been replaced by dolomite (text-fig. 5B), producing pseudomorphs.

A-2- Sandy bioclastic grainstone

There are beds composed of skeletal debris including echinoderms and brachiopods. Quartz grains represent 10% to 15% of the non-skeletal components. This facies was occurs at the base of the Khan Formation, and it marks the beginning of its carbonate deposition, and during the highstands (text-fig. 5C).

A-3- Sandy intraclast grainstone

This facies consists of a dark gray, medium-bedded grainstone of sub-rounded to rounded intraclasts with loose packing. Fine- to coarse-grained, moderate to well sorted, sub-rounded to rounded mono-crystalline quartz grains represents about 10% to 15% of the rock. This facies was observed near the base of the Khan Formation (text-fig. 5D).

A-4- Sandy ooid grainstone

This facies consists of a light gray, medium-bedded, fine- to coarse grained oolitic grainstone. The moderately- to well-sorted ooids form 70% of this facies with 10% to 15% of poorly sorted, angular, medium sand-sized quartz. The skeletal debris, as a minor component of this facies, includes brachiopods and bivalves. This facies was observed at the base of the Khan Formation (text-fig. 5E).

A-5- Quartz sandstone

The quartz sandstone facies consists of brownish gray, medium beds of fine- to coarse-grained, moderately to poorly sorted, angular to sub-rounded, sand-sized mono-crystalline quartz. Quartz grains form 90% of this facies. The skeletal fragments are less than 5% of the minor constituents. Also, there is common trough and planar cross-bedding (text-fig. 5F).

Interpretation

The dolomitized micrite and dolomudstone with birdseye and gypsum/anhydrite casts were deposited in the supratidal to upper intertidal sub-environments. The sandy intraclast/ooid grainstone was deposited in a high energy, upper intertidal sub-environment, which is supported by the lack of micrite and

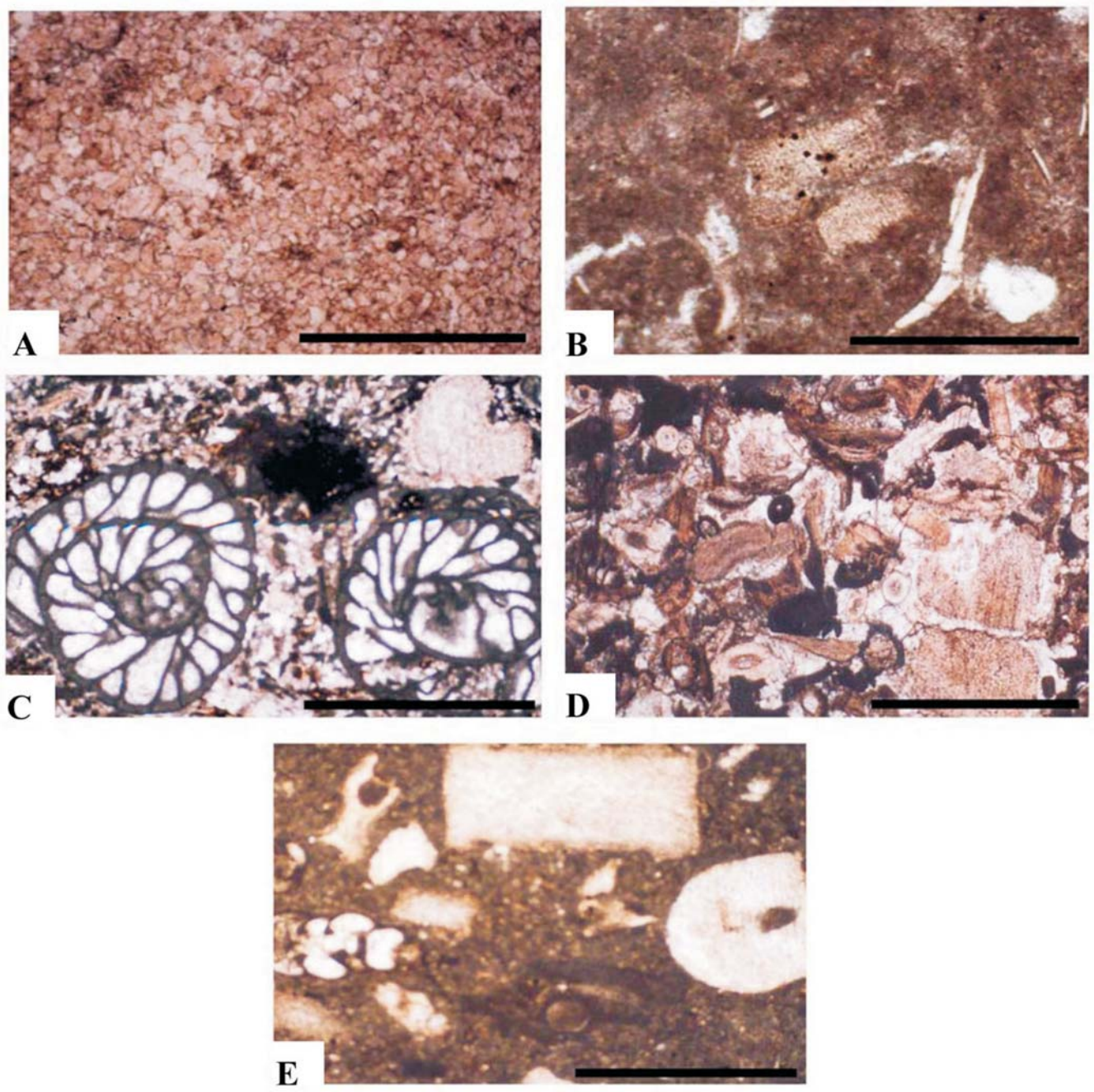

TEXT-FIGURE 6

A Photograph of the dolosparite of the Khan Formation.

B-C, Photomicrographs of the lagoonal facies of the Khan Formation.

B Bioclastic wackestone showing crinoid stem and bivalve fragments.

C Fusulinid bioclastic grainstone showing poorly sorted grainstone with fusulinid and crinoid stem fragments.

D Photomicrograph of the shoal facies of the Khan Formation, with bioclast packstone/grainstone illustrating grain supported packstone/grainstone, with common crinoid stems and brachiopod fragments.

E Photomicrograph of the open marine facies of the Khan Formation's bioclastic wackestone/packstone showing a crinoid stem fragment and a smaller foraminifer shell in a micritic matrix. Scale bar is 0.1mm.

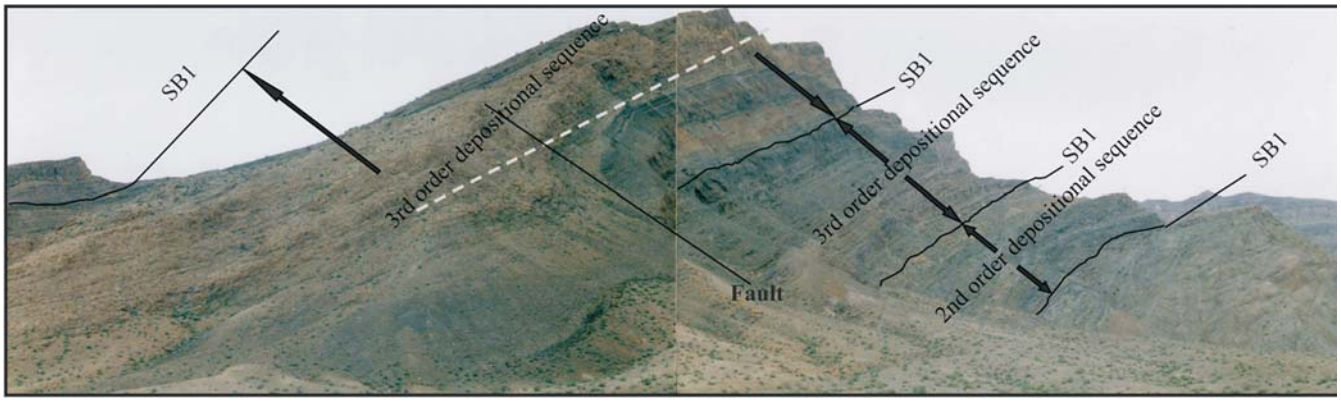

TEXT-FIGURE 7
The Khan Formation at the Halvan location showing the sequence boundaries and the depositional sequences, with the view toward the southwest.

vertical association with lagoonal and proximal tidal flat facies (Shinn 1983). The high compositional and textural maturity in the Khan Formation quartz arenite, as well as flaser bedding, cross-bedding and laminations indicate a high energy depositional environment for this facies. Vertical grading of the quartz arenite to lithic sandstone, flaser bedding, herringbone cross-bedding, and a vertical association of the clastic facies with carbonate tidal facies point to sedimentation in a shallow supratidal to an upper intertidal environment. In some outcrops, the quartz arenites were replaced by local conglomerates. This conglomerate has angular pebble and cobble clasts that indicate these clasts were proximal to their source area(s).

A-6- Diagenetic dolomite

There are three types of dolomite crystals that were identified in the Khan Formation on the basis of their textural changes, internal structure and crystal shape. These are very fine crystalline dolomites or dolomicrites, fine crystalline dolomites or dolomicrosparites and medium crystalline dolomites or dolosparites. Dolomitization and dolomites are very common throughout the Khan Formation. Dolomite bed thicknesses are variable.

Dolomicrite. Dolomite crystals show xenotopic fabric and are fully dense and have no porosity. The relics of original allochems are also present (including crinoid stems and brachiopod shells). The size of the dolomite rhombs ranges between 5 to 16 microns (with a mean of 11 microns) (text-fig. 5G).

Dolomicrosparite. These dolomites are subhedral to non-euhedral and have fabrics equal with hypidiotopic (Friedman 1965), idiotopic-s (Gregg and Sibley 1984) and planar-s (Mazzullo 1992). The crystal faces are of the planar-s type. They consist of 16-62 micron-sized crystals (with a mean of 40 microns) (text-fig. 5H).

Dolosparite These dolomites consist of anhedral crystals with non-planar faces and have a xenotopic fabric. The size of the dolomite crystals ranges from 62 to 270 microns (with a mean of 170 microns) (text-fig. 6A).

Interpretation

The dolomicrites are considered as syngenetic. They formed during very early diagenesis in supratidal and upper intertidal environments (Adabi 2004). Given the texture and fine crystals in the dolomites, the retention of the primary sedimentary structures such as birdseyes, and the presence of quartz grains scattered in the dolomicrites of the Khan Formation, these dolomites were formed under near-surface low temperature conditions (Sibley and Gregg 1987; Gregg and Shelton 1990). The dolomicrosparites are formed by the replacement of limestones or recrystalization of dolomicrites under critical temperatures (less than 60° C; Gregg and Shelton 1990; Mazzullo 1992). In the Khan Formation, the dolomicrosparites are the relics of allochems including brachiopod shells and intraclasts. The original sedimentary textures in the dolosparites of the Khan Formation are not preserved. The dolosparites are formed at very high temperatures and replace the limestones (Gregg and Sibley 1984; Sibley and Gregg 1987; Gregg 1988; Gregg and Shelton 1990).

It appears that the Khan Formation dolosparites formed as a result of a dolomicrosparite recrystallization or a displacement of primary limestones at a high temperature and during deep burial stages. The fabric change in the Khan Formation dolomites from a dolomicrite to a dolomicrosparite, followed by a dolosparite, indicates increasing alteration.

Lagoon sediments (facies B)

The lagoon sedimentary deposits are composed of a bioclastic wackstone/peloid bioclastic grainstone and a fusulinid bioclastic grainstone.

B-1- Bioclastic wackestone

The bioclastic wackestone consists of thin- to medium-bedded, light to dark gray beds of skeletal debris cemented by a micrite. The sparse skeletal fragments include fusulinids, medium-grained crinoid stems and brachiopods, ostracodes; and less than 5% smaller foraminifers are minor grains. The skeletal grains are relatively intact (text-fig. 6B).

B-2- Peloid bioclastic grainstone

The peloid bioclastic grainstone consists of medium-bedded, gray beds. The skeletal grains form 40% of this facies including foraminifers, echinoderms, brachiopods, bivalves, and dasyclad algae that are not closely packed with poor sorting. The oval peloids are about 10% to 15%.

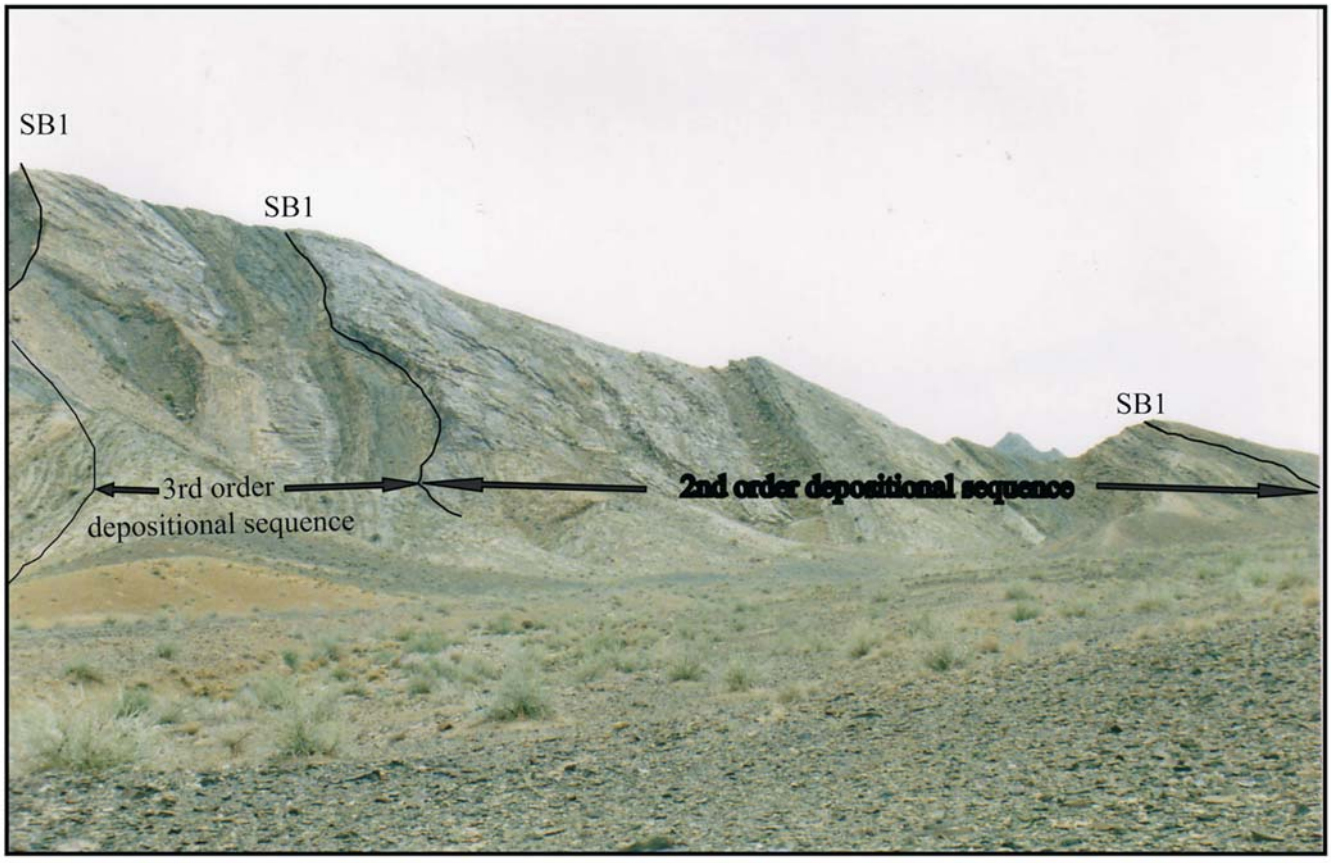

TEXT-FIGURE 8
The Khan Formation at the Rahdar section illustrating the sequence boundaries and the depositional sequences. Note the difference between the number of depositional sequences at the Halvan and Rahdar locations. View is toward the southwest.

B-3- Fusulinid bioclastic grainstone

This facies consists of medium- to thick-bedded gray beds with fusulinids, brachiopods and echinoderms that form 60% of this facies. The minor components are smaller foraminifers, dasyclad algae and ostracodes. The skeletal grains have micritized boundaries, and they were cemented by sparite (text-fig. 6C).

Interpretation

The relatively low diversity. a low abundance normal marine fauna, and the high proportion of micritic mud as well as the partial micritization of skeletal fragments in the bioclast wackestone suggest the deposition was in a quiet water and lagoonal environment (Wilson 1975; Hine 1977; Nichols 2000). This facies was deposited mainly in a sheltered lagoon environment with an open marine circulation under a low to moderate energy near shoals. It was locally deposited in a semi-restricted lagoon below the fair-weather wave base. This is supported by scour-and-fill structures in the field (Aigner 1982).

Shoal sediments (facies C)

The shoal sediments include a bioclastic packstone-grainstone and an intraclast bioclastic grainstone facies. The bioclastic packstone-grainstone shares similar features with the the same lithology in the Jamal Formation. The intraclast bioclastic grainstone consists of thick-bedded, gray, crinoids and brachiopods rich grainstone. Subrounded to rounded intraclast grains comprise 15% of the lithology.

Interpretation

The formation of a bioclastic packstone-grainstone (text-fig. 6D), an intraclast bioclastic grainstone, and their components (allochems and orthochems) are the same as those in the Jamal Formation shoal facies.

Open marine sediments (facies D)

Open marine sedimentary deposits include a bioclastic wackestone that grades upward to a bioclastic packstone facies. This open marine facies consists of dark gray, thin to medium beds of poorly sorted, skeletal grains including echinoderms, smaller foraminifers and brachiopods (text-fig. 6 E).

Interpretation

This facies is not found extensively in the Khan Formation sections, and it has some similar features with the shoal facies. However, the abundance of carbonate mud and the poorly sorted grains in this facies are indicative of a quiet-water and a low-energy environment. Considering its position over the shoal facies, an open marine setting is likely for this facies.

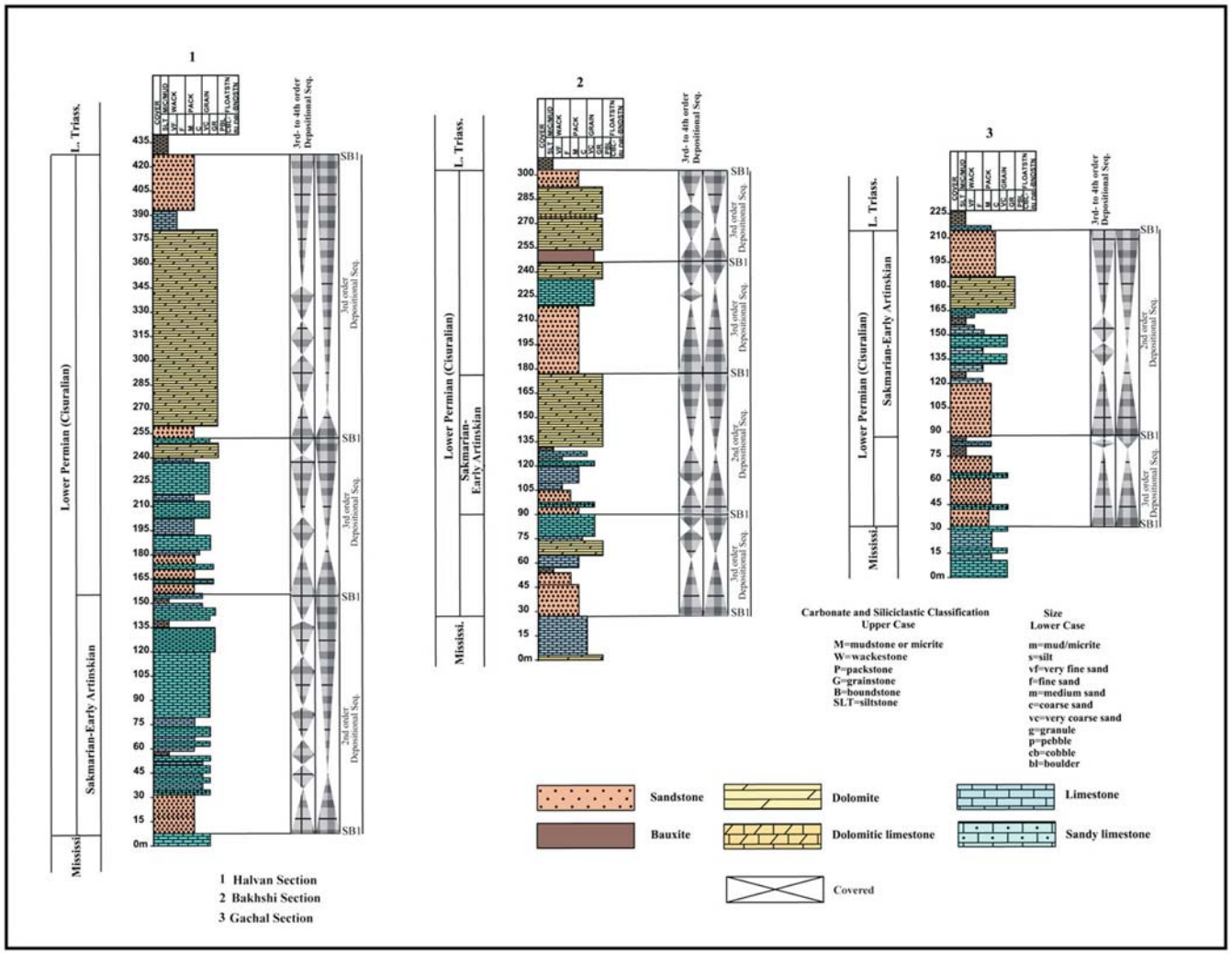

TEXT-FIGURE 9
Stratigraphy and the depositional sequences (second-, third-, and fourth-order) of the Khan Formation at the Halvan, Bakhshi and Gachal sections. The depositional sequences and related sequence boundaries (SBs) are identified. SB1: a type 1 sequence boundary.

DEPOSITIONAL MODEL

The depositional systems for the Jamal and Khan formations were different. The Jamal Formation deposition was on a homoclinal ramp (*sensu* Read 1982, 1985), particularly on an inner-ramp and mid-ramp (Wright 1986; Burchette et al. 1990). This is supported by the abundance of deposits characteristic of shoal, lagoon and tidal flat sediments, and lesser occurrences of graded beds, hummocky cross-stratification (HCS) and storm-related features.

In distally steepened ramps, as described by Tucker and Wright (1990) and Tucker et al. (1993), a slope break is situated between the outer ramp and the basin. Many of these include slumping and slope apron deposits, which are not present in the Jamal Formation. In the Jamal Formation inner-ramp, the deposits consist mostly of bioclastic and oolitic allochems that build shoal sediment bodies. The lagoonal facies show a variety of mud-, wacke- or packstone sediments. Computer simulations demonstrated that models with a uniform sediment production across ramps form more homoclinal morphologies (Elrick and Read 1991; Read et al. 1991). High oolitic production in shallow water characterizes ramp-dominated environments, which occur in the Jamal Formation, especially at the type section.

Although we propose a carbonate ramp model for the depositional environment of the Jamal Formation at its type section and the Bagh-e-Vang sections, there are some distinct differences among facies between them. The lagoon and shoal facies are more dominant in the type section than at the Bagh-e-Vang section. The lagoon sub-environment in the type section can be subdivided into three parts. The shoal and lagoon facies include ooid and bioclastic grainstones that follow lagoon facies through the formation. The mid-ramp facies does not occur in the type section.

On the other hand, the presence of the chert nodules and lenses with fossils including the radiolaria and/or calcispheres and the sponge spicules (D-2 microfacies, Jamal Formation) at the Bagh-e-Vang section represent deposition in the calmer water

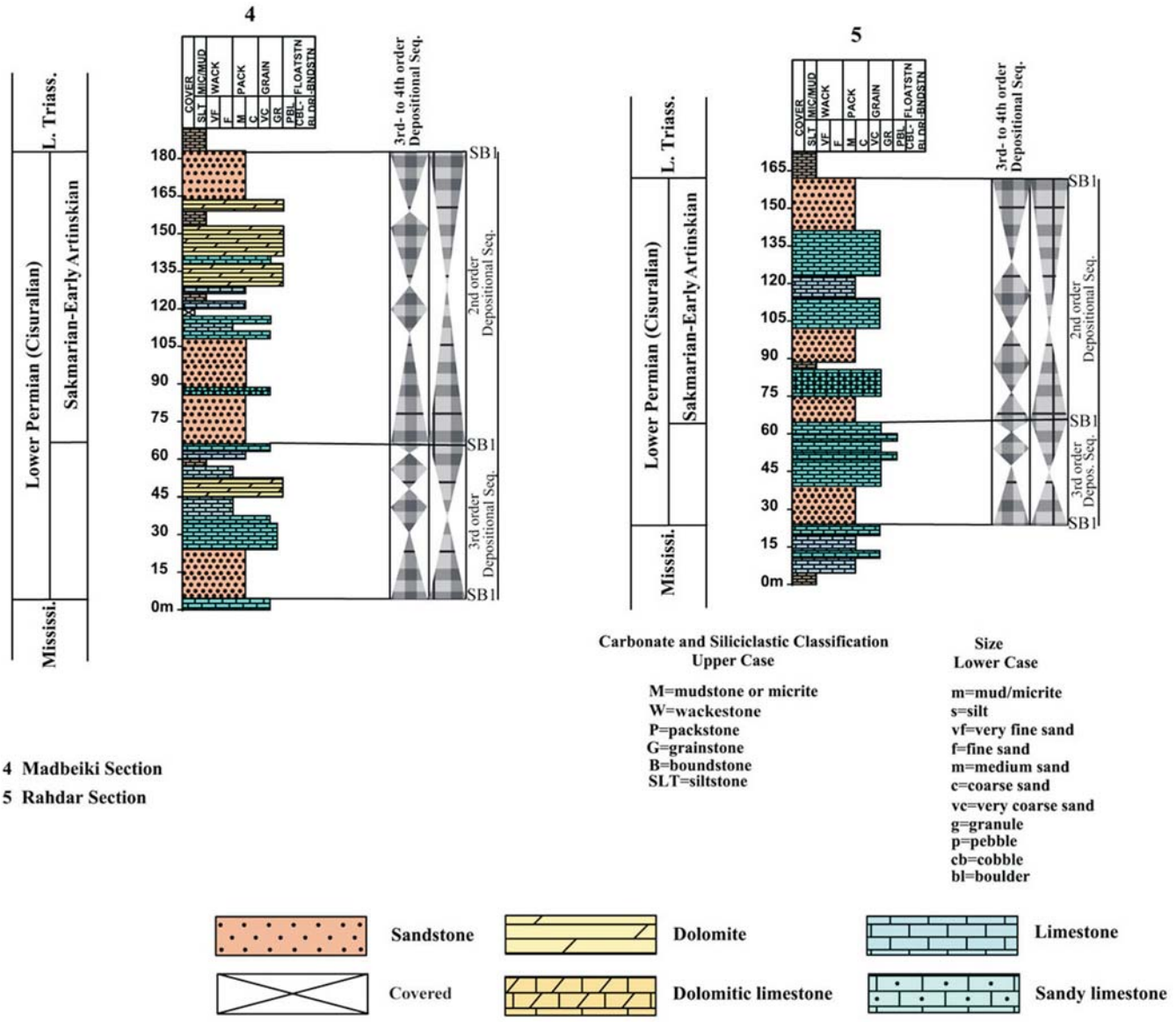

TEXT-FIGURE 10
Stratigraphy and the depositional sequences (second-, third-, and fourth-order) of the Khan Formation at the Madbeiki and Rahdar sections. The depositional sequences and the related sequence boundaries (SBs) are identified. SB1: a type 1 sequence boundary.

of the mid-ramp with some influence from the shallow ramp. This facies is common in Paleozoic and Mesozoic basinal carbonates, deeper shelf carbonates as well as in mid-ramp and outer-ramp settings (Flügel 2004).

The Kalmard Basin was characterized by cyclic sequences composed of thick siliciclastic deposits and relatively thin carbonate sediments during the Lower Permian. A shoreline environment with mixed siliciclastic-carbonate sediments describes the depositional setting of the Khan Formation. Globally, the Permo-Carboniferous rocks contain especially good examples of mixed siliciclastic-carbonate sequences (Mack and James 1985). The accepted sedimentary environment model for mixed siliciclastic and carbonate deposition involves shelves in which clastic sediments are trapped in the near shore zone with simultaneous deposition of carbonate sediments in clear, deeper-water subtidal, as well as intertidal settings (Myrow and Landing 1992).

The tidal flat facies are widespread in the Khan Formation. The carbonate allochems significantly increase upwards, reflecting diminished siliciclastic input as sea level rose and *in situ* carbonate production increased. These carbonate facies are subdivided into the lagoon and shoal sub-environments and a very rare open marine facies. They are capped by a tidal flat facies. Bauxite deposits record subaerial exposure.

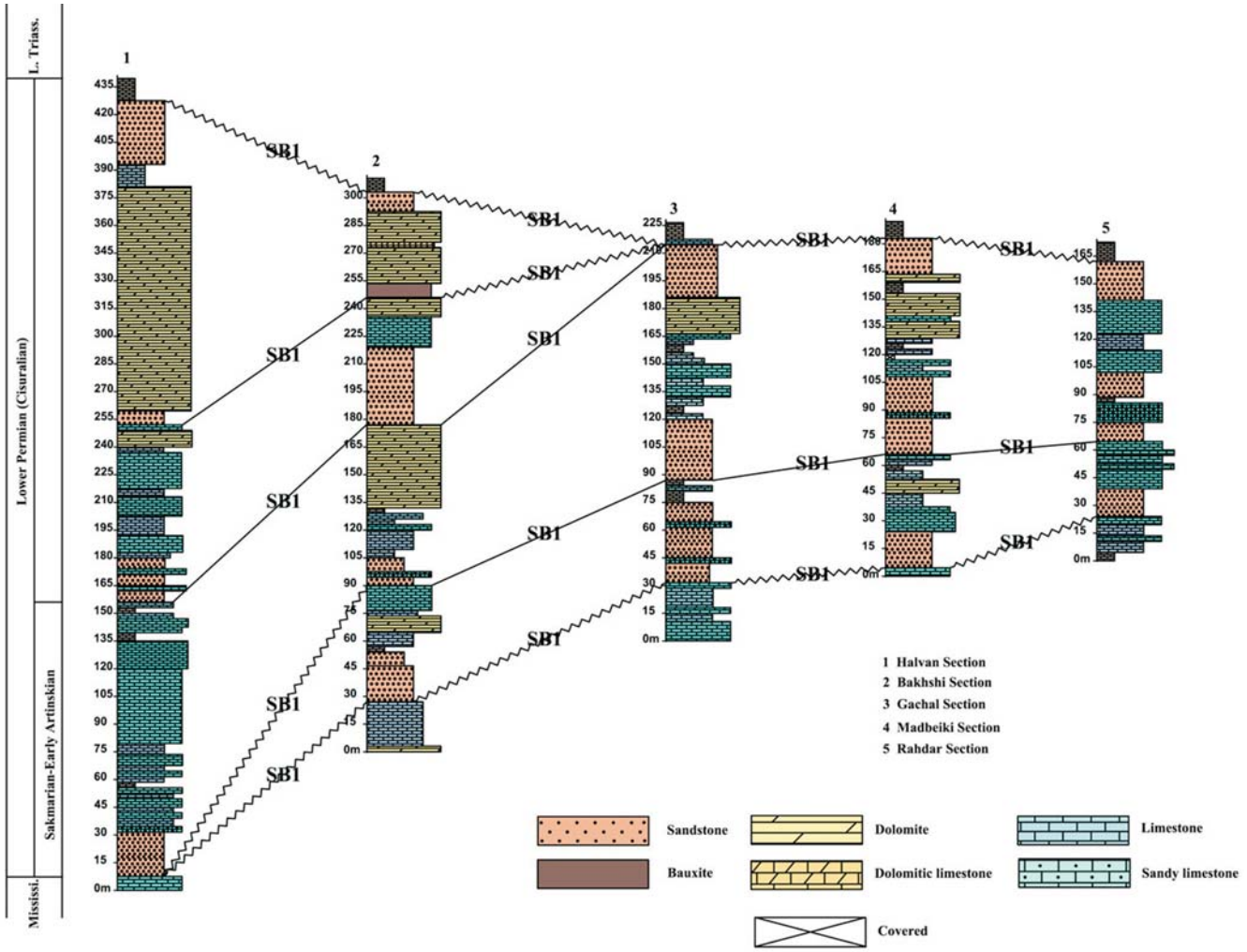

TEXT-FIGURE 11
Correlation of the depositional sequences in the Khan Formation between the Halvan, Bakhshi, Gachal, Madbeiki and Rahdar outcrop sections in the Kalmard area.

DEPOSITIONAL SEQUENCE

Khan Formation

The Lower Permian (the Sakmarian to the early Artinskian in age) Khan Formation in the Kalmard basin displays a cyclic sedimentation (text-figs. 7, 8, 9, 10). Like other mixed siliciclastic-carbonate depositions, the sequence cyclicity in the Khan Formation is commonly observed elsewhere (Mack and James 1985; Myrow and Landing 1992; Barnaby and Ward 2007; Lubeseder et al. 2009). The asymmetric parasequences reveal a vertical facies change commensurate with a seaward progradation of the shoreline. The Khan Formation can be divided into second- and third-order, shallowing-upward depositional sequences. Each sequence records a transgression and a regression.

Sequence 1 is a third order cycle and was deposited at the Bakhshi, Rahdar, Madbeiki, and Gachal locations, and it is missing at the Halvan section (text-figs. 7, 8, 9, 10). The LST deposits of the Sequence 1 include quartz sandstones. These siliciclastic deposits are also included in the lower part of the TST (text-figs. 9, 10). The transgressive system tract in Sequence 1 is composed mainly of a lagoonal facies. The HST deposits are recognized by a shallowing-upward progradational stacking pattern, which mostly includes a subtidal facies with a more restricted fauna. The lower and upper boundaries of Sequence 1 are both a type 1 at the sections mentioned above (text-figs. 7, 8, 11).

Like Sequence 1, Sequence 2 (second-order cycle) begins with LST sedimentary deposits composed of sandstones and are included in the lower part of the TST (text-figs. 9, 10). The TST is characterized by a bioclastic packstone, a bioclastic ooid grainstone, an intraclastic grainstone, and a bioclastic wackestone/packstone. The MFS is marked by fusulinid- rich beds. The transition from the lagoon to mainly a tidal flat facies indicates a sea level fall, gradual shallowing conditions, and a reduced accommodation during the HST. The HST deposits are indicated by a progradation of the tidal flat facies over a lagoon and a foreshore facies. The lower and upper boundaries of Sequence 2 are both a type 1.

TEXT-FIGURE 12
The Jamal Formation at the Jamal location showing the sequence boundaries and the depositional sequences. View is toward the north.

The transition from the Sequence 2 to Sequence 3 (third-order cycle) is accompanied by a major change from a humid/temperate to an arid climate, as well as a switch to continental conditions. This is inferred from a transition of sandstones containing plant remains to bauxite. Sequence 3 was deposited at the Bakhshi and Halvan sections. The LST deposits included in the lower part of the TST are composed of sandstones. The TST at Halvan is characterized by a bioclastic wackestone, an intraclastic grainstone, and a bioclastic packstone containing algae, *Tubiphytes*, echinoderms, crinoids and brachiopods. At the Bakhshi section, a TST is indicated by a dolomitized bioclastic wackestone/packstone, a dolomitized ooid grainstone, a dolomitized wackestone that are interpreted to indicate lagoon to fore-shoal environments. The HST is missing at the Bakhshi section, and it is thin and composed of tidal flat facies at the Halvan section. The upper boundary of the Sequence 3 is a type 1.

Sequence 4 (third-order cycle) is represented only at the Halvan section. This sequence starts with sandstones of a lowstand transgressive system tract. The TST deposits are characterized by an aggradational stacking pattern. The HST sediments are indicated by four shallowing-upward and thinning progradational parasequences. The upper boundary of the Sequence 4 is a type 1.

The upper boundary of the Khan Formation defines a significant disconformity that is related to epeirogenic movements after the deposition of the Khan Formation at the end of the Sakmarian to the early Artinskian stages. This disconformity is widespread and very useful for correlation. After deposition of the Khan Formation, the Kalmard area witnessed a significant regression. From the late Early Permian through Early Triassic time this area was subaerially exposed, as evidenced by the bauxite horizons at the top of the Khan Formation.

Jamal Formation

The Middle Permian Jamal Formation in the Shotori area consists of three third-order shallowing-upward depositional sequences (text-figs. 12, 14). The depositional Sequence 1 (lower Roadian in age) was deposited during a transgression over the Carboniferous Sardar Formation siliciclastics. The TST deposits are characterized by open-marine, fore-shoal and lagoon facies and show an aggradational parasequence stacking pattern. The MFS is indicated by bioclastic grainstones which are composed completely of brachiopods and crinoids. The HST shows transition from lagoon to tidal flat environments. The shallowing-upward trend from shoal/lagoon to supratidal facies is characteristic of a progradational stacking pattern during highstand system tract (HST). Also the presence of lime

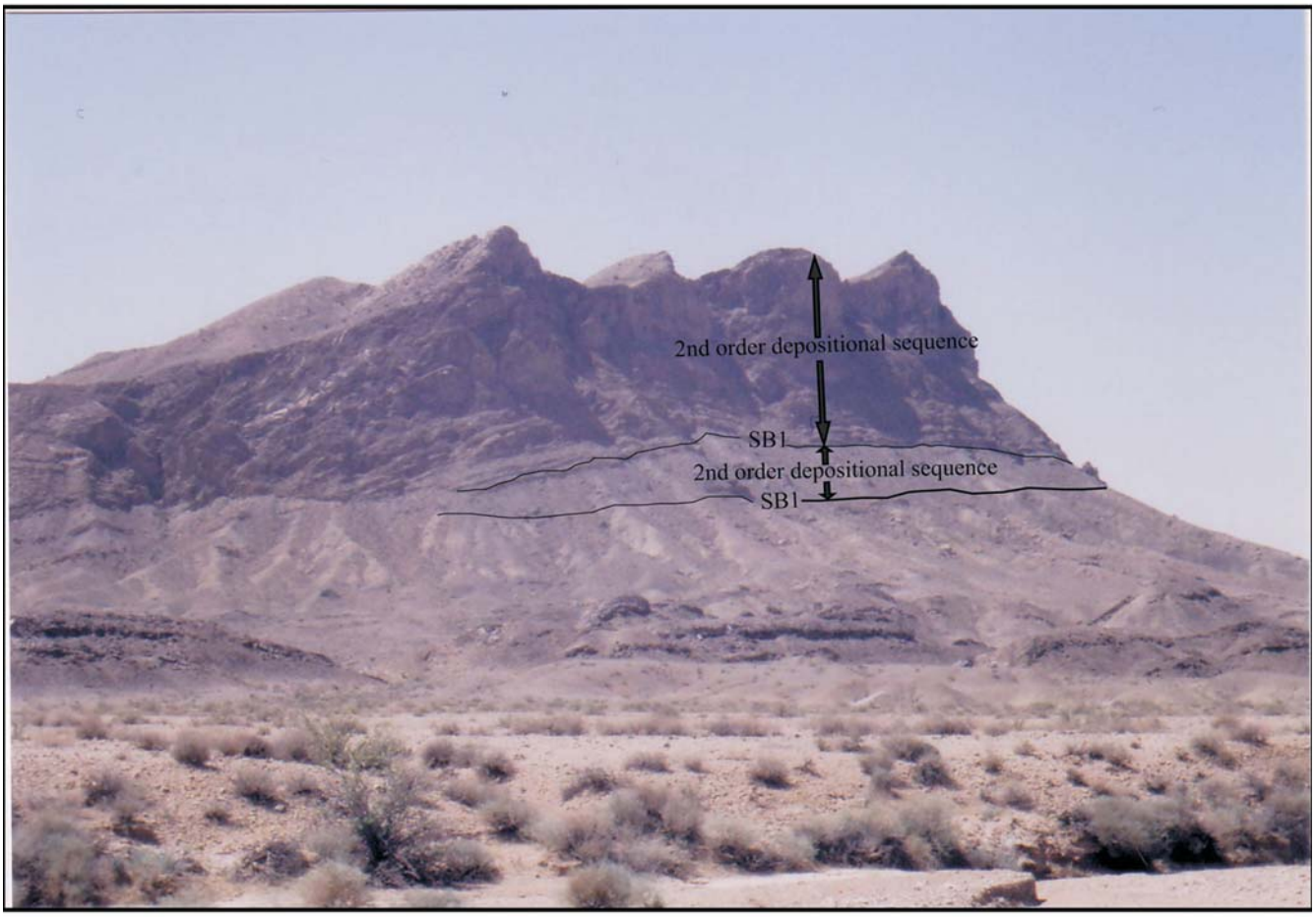

TEXT-FIGURE 13
The Jamal Formation at the Bagh-e-Vang section, illustrating the sequence boundaries and depositional sequences; view is toward the north.

mudstone, dolomudstone with calcite pseudomorphs after gypsum/anhydrite, birdseye structures, and quartz sand are interpreted to indicate a progressive progradation during the late HST and subaerial exposure. The lower and upper boundaries of the Sequence 1 are both a type 1 (text-figs. 12, 15).

The Sequence 2 of the upper Roadian Stage is similar to Sequence 1, in that the TST deposits are succeeded by the lagoonal and shoal parasequences of the HST deposits. The transgressive system tract of the Sequence 3 (the Wordian to the Capitanian in age) is composed of a bioclastic wackestone, an intraclastic grainstone, an intraclast oncoid grainstone and a bioclastic wackestone/packstone. A retrogradational stacking pattern is indicated by thickening-upward facies which changes from a intraclastic grainstone, and a dolomitized ooid grainstone to a crinoid, fusulinid, brachiopod packstone. The MFS is recognized by bioclastic wackestone/packstone that contains an open marine facies. The HST is characterized by a transition from an open marine to a shoal, a lagoon and ultimately a tidal flat facies. The dolomitic limestones appear in the uppermost portion of the Jamal Formation. The abundance of the ooid grainstone and the lagoon and the tidal flat facies indicate a remarkable reduction in accommodation rate. The lower boundary of the Sequence 3 is a type 1. The upper boundary of the Jamal Formation in this section is faulted with the Lower Triassic Sorkh shale Formation.

The Artinskian to the early Wuchiapingian in age Jamal Formation in the Bagh-e-Vang section in the Shirgesht area consists of two second order and one third-order depositional sequences (text-figs. 13, 14). The first sequence (the Artinskian to the Kungurian in age) is a second-order cycle that was deposited over the Carboniferous Sardar Formation sandstones. The lower contact of the Jamal Formation with the Sardar Formation is a widespread disconformity in the study area. It is a major sequence boundary and a transgressive surface. The TST deposits of Sequence 1 are characterized by a bioclastic grainstone, a bioclastic peloid grainstone and a bioclastic wackestone/packstone, with both containing algae, echinoderms, gastropods, corals, brachiopods and fusulinids. It is interpreted as including a lagoon to an open marine environment. In the middle part of this sequence, there are fine-grained siliciclastics interbedded with limestones that decrease upwards. The MFS is characterized by a bioclastic packstone, with fusulinids, algae, and echinoderms. The HST is composed mainly of a lagoon facies with restricted fauna and tidal flat deposits, showing a progradational stacking pattern. The upper sequence boundary of Sequence 1 is a type 1 (text-figs. 13, 15). There is no evi-

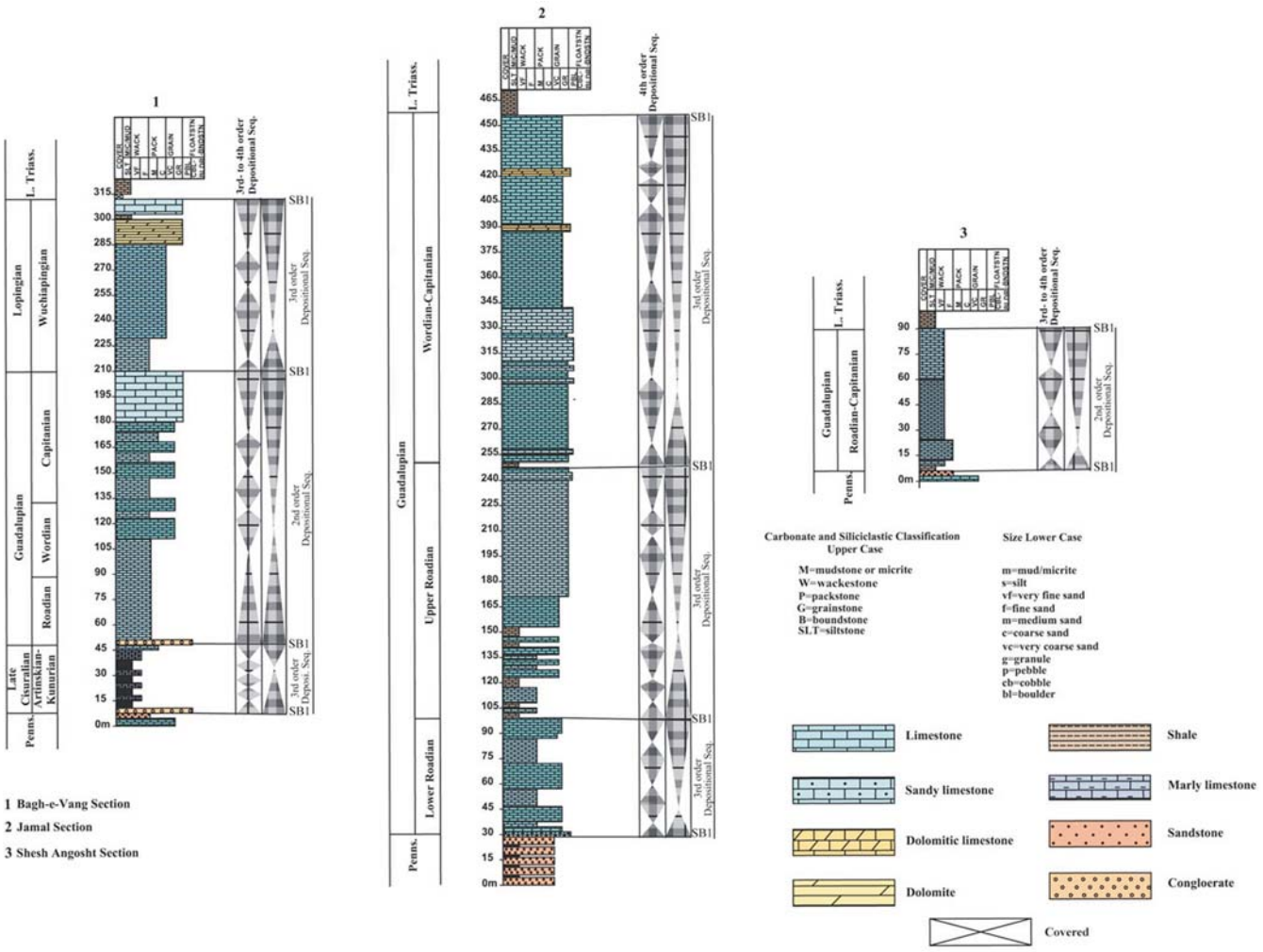

TEXT-FIGURE 14
Stratigraphy and depositional sequences (second-, third-, and fourth-order) of the Jamal Formation at the Bagh-e-Vang, Jamal and Shesh Angosht sections. The depositional sequences and the related sequence boundaries (SBs) are identified. SB1: a type 1 sequence boundary.

dence of the Sequence 1 deposits in western outcrops (Shesh Angosht location).

Although there is a local conglomerate at the base of the Sequence 2 (second-order cycle) at the Bagh-e-Vang section, the boundary between Sequences 1 and 2 is marked by a significant deepening and a conspicuous shift in the depositional environment. The HST deposits of the Sequence 1 are characterized by several shallowing- and thickening-upward parasequences. These parasequences formed in a mid ramp setting and are not followed by shallower facies. Therefore, they are indicative of a progressive progradation of the mid-ramp toward deeper waters. The absence of a shallow water fauna and the presence of sponge spicules, radiolaria and/or calcispheres support a TST interpretation. HST deposits include the thickening and coarsening-upward parasequences that show aggradational and progradational normal marine packstone and grainstone cycles. The upper boundary of Sequence 2 is type 1. The TST and HST deposits at the Sheshangosht section are very thin, and they do not include a mid-ramp facies in this section.

Sequence 3 (third-order) of the early Wuchiapingian Stage is composed of three thickening-upward parasequence sets with the presence of sponge spicules, calcispheres, and possible radiolaria. The HST deposits in the Sequence 3 are characterized by abundant benthic organisms and a marked increase in carbonate production. The MFS is marked by a transition from an open marine facies to a shelf margin facies. The upper boundary of the Sequence 3 is a type 1 with the Lower Triassic Sorkh shale Formation. The Sequence 3 was not deposited at the Shesh Angosht section.

The Sequence 1 (the Artinskian to the Kungurian in age) of the Jamal Formation at the Bagh-e-Vang section was not deposited at its type section in the Shotori area. Also Sequence 2 (the Roadian to the Capitanian in age) at the Bagh-e-Vang section is comparable with the Sequence 1 (also the Roadian to the Capitanian in age) at the Jamal Formation type section.

DISCUSSION

The Carboniferous and Lower Permian glaciations covered extensive areas of Gondwana (Crowell 1978; Isbell et al. 2003). They have been considered as a driving force for cyclicity of Permo-Carboniferous rocks in many parts of the world (Boardman and Heckel 1989; Dickinson et al. 1994; Heckel 1994). Isbell et al. (2003) proposed that Gondwana glaciation was less widespread during Permian time, and therefore that glacio-eustatic fluctuations were smaller than previously hypothesized. As well as possible glacio-eustactic controls on sea level, the development of accommodation space through tectonic activity strongly influenced the accumulation of the carbonate rocks in both the Tabas and Kalmard regions.

Distinguishing tectonic versus eustatic sedimentation cyclicity has been addressed in Batt et al. (2007), and Grader et al. (2008) in two late Paleozoic sequences deposited in active tectonic areas that serve as proxies for the glaciations. Tectonic accommodation produced sections much thicker than coeval ones that were less affected by tectonics. Nevertheless, even in those sections affected by tectonics, the authors demonstrated that eustatic cyclicity quickly overprints upper parts of the depositional cycles.

In east-central Iran, it is clear from overall sedimentary thicknesses that significant accommodation was provided tectonically. These effects were more significant in some sections than other, coeval sections. Regardless of tectonic influence, eustatic cyclicity is evident in all sections, as the carbonate factory always exceeded rate of subsidence.

Text-figsures 11 and 15 delineate Khan and Jamal formation biostratigraphic ages, respectively, and they also delineate the timings of tectonic subsidence and generation of accommodation space. Biostratigraphic data suggest that subsidence occurred in Sakmarian time, producing accommodation space for the Khan Formation.

Eustatic cyclicity is evident in all sections of the Khan Formation, because each section records a sequence boundary in the same relative stratigraphic position. Parasequences correlate well across the depositional transect. Each has a sandstone to thin-bedded subtidal carbonate, to more offshore shelly bank in its TST sequence. The Khan Formation was subsequently partly eroded.

The Jamal Formation has a relatively similar cyclic development as the Khan Formation. That is, after significant subsidence and accommodation in late Cisuralian time, longer-term (third-order) cyclicity commenced after a long hiatus of subaerial exposure and non-deposition. Parasequences are different from those in the Khan Formation, in that there are fewer sandstone beds to mark initial beds of parasequences. The Jamal section shows the most accommodation space, relative to the Bangh-e-Vang and the Shesh Angosht sections. However, all have parallel parasequences developed within the more subtle changes from a carbonate mudstone and a wackestone through a packstone. Towards the top of the Jamal Formation are dolomitic units, signifying cyclic HSTs reaching a stagnant sea surface with evaporation. Triassic subaerial exposure provided an erosional top to the Jamal Formation.

Owing to the lack of more detailed biostratigraphic zonations, assigning specific biostratigraphic ages to possible glacially-caused eustatic cycles in both the Tabas and the Kalmard regions remains difficult. With more precise biostratigraphic data in Permian sections in Iran (e.g. in the Alborz and Zagros mountains) better proxies for Gondwana glaciation may be demonstrated.

CONCLUSIONS

1. The Khan Formation in the Kalmard area (within the Posht-e-Badam block) was deposited in a nearshore environment. The Lower-Upper Permian deposits of the Jamal Formation in the Shotori and Shirgesht areas (within the Tabas block) were deposited on a homoclinal carbonate ramp showing a deeper water facies in the northern sections (Bagh-e-Vang section) relative to the southern locations.

2. The Khan Formation is represented by second- and third-order cyclic sequences of thick siliciclastic deposits and thin carbonates. The Lower-Upper Jamal Formation sections show second- and third-order shallowing-upward carbonate sequences.

3. The principal control of the cyclic development in both the Khan and the Jamal formations cannot be exclusively attributed to Gondwana glaciation because of imprecise biostratigraphic data. We suggest that the cyclicity in the Permian was initially a product of local tectonic loading producing accommodation space, with a eustatic overprint.

ACKNOWLEDGMENTS

The authors thank the three reviewers for their constructive comments on this paper. Further, we wish to thank editor Mark Williams for very careful editing of the final draft.

REFERENCES

ADABI, M. H., 2004. A re–evaluation of aragonite versus calcite seas, Carbonates and Evaporites, 19 (2), 133–141.

AGHANABATI, A., 1977. *Étude géologique de la region de Kalmard (W. Tabas)*. Tehran: Geological Survey of Iran. Report 35, 230 pp..

———, 2004. *Geology of Iran.* Tehran: Geological Survey of Iran. 586 pp. (in Farsi)

AINGER, T., 1982. Calcareous Tempestites: Storm–dominated Stratification in Upper Muschelkalk Limestones (Middle Triassic, SW–Germany). In: Einsele, G. and Seilacher, A., Eds., *Cycle and event stratigraphy,* 180–198. New York, Berlin–Heidelberg: Springer Verlag.

AlAVI, M., 1991. *Tectonic map of the Middle East.* Tehran: Geological Survey of Iran.

AREFIFARD, S., 2006. "Microbiostratigraphy and Microfacies of Permian Deposits in Kalmard, Shotori and Shirgesht areas (East–Central Iran)", Unpubl. Ph. D. Thesis, Shahid Beheshti University, Tehran, 252 pp.

ARFANIA, R. and SHAHRIARI, S., 2009. Role of southeastern Sanandaj–Sirjan Zone in the tectonic evolution of Zagros Orogenic Belt, Iran. *Island Arc,* 18: 555–576.

BAGHBANI, D., 1993. The Permian sequence in the Abadeh region, Central Iran. In: Koroteev, A. V., Ed., *Contributions to Eurasian geology,* 7–22.. Columbia: Univerrsity of South Carolina: Occcasional Publication of the Earth Sciences Research Institute, 9B.

———, 1997. Correlation charts of selected Permian strata from Iran. *Permophiles,* 30: 24–25.

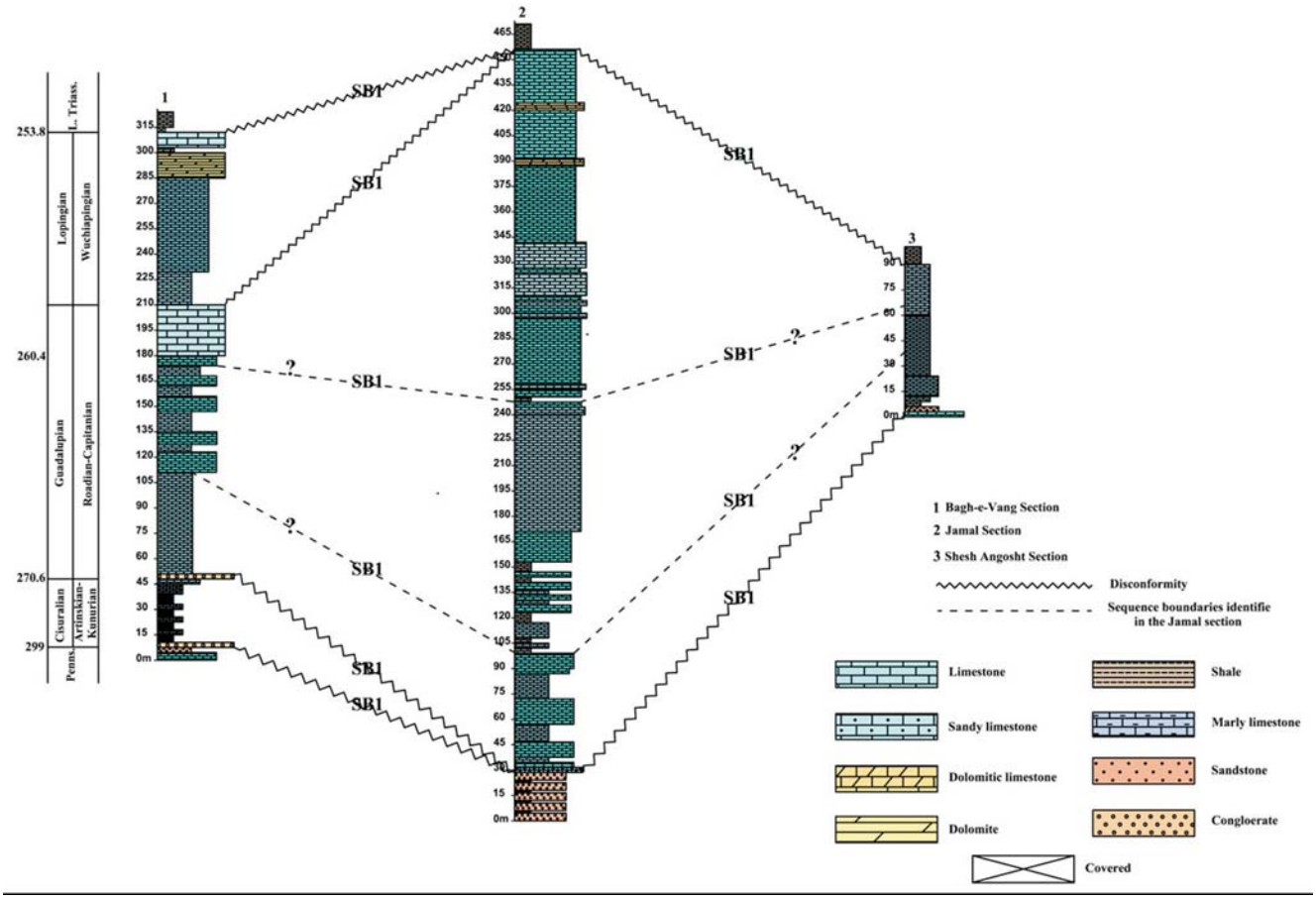

TEXT-FIGURE 15
Correlation of the depositional sequences in the Jamal Formation between the Bagh-e-Vang, the Shesh Angosht (Shirgesht area), and the Jamal (Shotori area) outcrop sections.

———, 1988. Shanita zone and its biostratigraphic significance in south and southwest Iran. *Review Paleobiology, Special Volume 2 "Benthos' 1986",* Part 1: 3-7

BARNABY, R. J. and WARD, W. B., 2007. Outcrop analog for mixed siliciclastic–carbonate ramp reservoirs–stratigraphic hierarchy, facies architecture, and geologic heterogeneity: Grayburg Formation, Permian basin, U. S. A. *Journal of Sedimentary Research,* 77: 4–58.

BATT, L. S., POPE, M. C., ISAACSON, P. E., MONTANEZ, I. P. and ABPLANALP, J., 2007. Late Mississippian Antler foreland basin carbonates and siliciclastics, east–central Idaho and southwestern Montana: distinguishing tectonic and eustatic controls. In: Lukasik, J. and Simo, T. T., Eds., *Controls on carbonate platform and reef development*, 147–170. Tulsa: Society of Sedimentary Geology. Special Publication 89.

BERBERIAN, M., 1983. Generalized tectonic map of Iran. In Berberian, M., Ed., *Continental deformation in the Iranian Plateau,* 52. Tehran: Geological Survey of Iran, Contribution to Seismotectonics of Iran, Part IV.

BERBERIAN, M., and KING, C. C. P., 1981. Toward a paleogeography and tectonic evolution of Iran. *Canadian Journal of Earth Sciences*, 18: 210–265.

BOARDMAN, D. R. and HECKEL, P. H., 1989. Glacial–eustatic sea–level curve for early Late Pennsylvanian sequence in north–central Texas and biostratigraphic correlation with curve for midcontinent North America. *Geology*, 17: 802–805.

BOZORGNIA, F., 1973. *Paleozoic foraminifersl biostratigraphy of central and east Alborz mountains, Iran:* Tehran: National Iranian Oil Company. Geological Labratory Publication 4, 185 pp.

BRUNET M–F, GRANATH J. W. and WILMSEN M., 2009. South Caspian to Central Iran basins: introduction, In: Brunet, M.-F., Wilmsen, M., and Granath, J.W., Eds., *South Caspian to Central Iran Basins, 1–6*. London: The Geological Society. Special Publication 312.

BURCHETTE, T. P., WRIGHT, V. P. and FAULKNER, T. J., 1990. Oolitic sandbody depositional models and geometries, Mississippian of southwest Britain: implications for petroleum exploration in carbonate ramp settings. *Sedimentary Geology,* 68, 87–115.

ÈADJENOVIÈ, D., RADULOVIÈ, N., OSTOJIÈ, Z. and MILUTIN, J., 2005. Jurske Formacije platoa Rumije (Crna Gora). *XIV Kongres geologa Srbije i Crne Gore, Novi Sad*, 186–192.. Beograd: Serbian Geological Society./

CROWELL, J. C., 1978. Gondwana glaciation, cyclothems, continental positioning, and climate changes. *American Journal of Science*, 278: 1345–1372.

DAVYDOV, V. I. and AREFIFARD, S., 2007. Permian fusulinid fauna of Peri–Gondwand affinity from the Kalmard region, East–Central Iran and its significance for tectonics and paleogeography. *Paleontologia Electronica,* 10-10A , 40 pp.

DERCOURT, J., RICOU, L. E. and VRIEL YNCK, B., 1993. *Atlas Tethys Paleoenvironmental Maps*. Paris: Gauthier–Villars, 307 pp.

DICKINSON, W. R., SOREGHAN, G. S. and GILES K. A., 1994. Glacio–eustatic origin of Permian–Carboniferous stratigraphic cycles: evidence from the southern cordilleran foreland region. In: Dennison, M. and Ettinson, F. R., Eds., *Tectonic and eustatic controls on sedimentary cycles*, 25–34. Tulsa: SEPM (Society of Sedimentary Geology). Concepts in Sedimentology and Paleontology, 4

ELRICK, M. and READ, J. F., 1991. Cyclic–ramp–to–basin carbonate deposits, Lower Mississippian, Wyoming and Montana: a combined field and computer modelling study. *Journal of Sedimentary Petrology*, 61: 1194–1224.

FLÜGEL, E., 1982. Microfacies Analysis of Limestones, Heidelberg, Springer–Verlag, 633 pp.

———, 2004. *Microfacies of carbonate rocks, analysis, interpretation and application,* Berlin, Springer–Verlag, 976 pp.

FRIEDMAN, G. M., 1965. Terminology of crystallization textures and fabrics in sedimentary rocks. *Journal of Sedimentary Petrology,* 35: 643–655.

GAETANI, M., ANGIOLINI L., KATSUMI, U., NICORA, A., STEPHENSON, M. H., SCIUNNACH, D., RETTORI, R., PRICE G. D. and SABOURI, J., 2009. Pennsylvanian–Early Triassic stratigraphy in the Alborz Mountains (Iran). In: Brunet, N.-F., Wilmsen, M., and Granath, J.W., Eds., *South Caspian to Central Basins,* 79–128, London: The Geological Society. Special Publication 312.

GHAVIDEL–SYOOKI, M., 184. Palynological study and age determination of Faraghan Formation in Kuh–e– Faraghan, Southeast Iran, *Bulletin of Faculty of Science of University of Tehran* 13, 41–46 (in Farsi, with English abstract).

GORGIJ, M. N., 2002. "Biostratigraphy and Sequence stratigraphy of Carboniferous Deposits in Central Iran", Unpubl. Ph. D. Thesis, Isfahan University, 410 pp.

GRADER, G. W., ISAACSON, P. E., DIAZ–MARTINEZ, E. and POPE, M. C., 2008. Pennsylvanian and Permian Sequences in Bolivia: Direct Responses to Gondwana Glaciation. In: Fiedler, G, C. R, Frank, T. D. and Isbell, J. L., Eds., *The Late Paleocoic Gondwanan Ice Age: Timing, extent, duration and stratigraphic records,* , 143–160. Boulder: Geological Society of America. Special Paper 441.

GREGG, J. M., 1988. Regional epigenetic dolomitization in the Bonneterre Dolomite (Cambrian), southeastern Missouri. *Geology*, 13: 503–506

GREGG, J. M. and SIBLEY, D. F., 1984. Epigenetic dolomitization and the origin of xenotopic dolomite texture. *Journal of Sedimentary Petrology*, 54: 908–931.

GREGG, J. M. and SHELTON, K. L., 1990. Dolomitization and dolomite neomorphism in the back reef facies of the Bonneterre and Davies Formation (Cambrian), southeastern Missouri. *Journal of Sedimentary Petrology*, 60: 495–562.

HAFTLANG, R., 1998."Stratigraphy of Upper Paleozoic rocks in Kalmard area," Unpubl. M. Sc. Thesis, Azad Universty, Tehran, 215 pp.

HECKEL, P. H., 1994. Evaluation of evidence for glacio–eustatic control over marine Pennsylvanian cyclothems in North America and consideration of possible tectonic effects. In: Dennison, M. and Ettinson, F. R., Eds., *Tectonic and eustatic controls on sedimentary cycles*, 25–34. Tulsa: SEPM Society of Sedimentary Geology. Condcepts in Sedimentology and Paleontology No. 4.

HINE, A. C., 1977. History of an active oolite sand shoal. Lily Bank, Bahamas. *Journal of Sedimentary Petrology*, 47: 1544–1581.

INSALACO, E., VIRGONE, A., COURME, B., GAILLOT, J., KAMALI, M., MOALLEMI, A., LOTFPOUR, M. and MONIBI, S., 2006. Upper Dalan member and Kangan Formation between the Zagros Mountains and offshore Fars, Iran: depositional system, biostratigraphy and stratigraphic architecture. *GeoArabia*, 11: 75–176.

ISBELL, J. L., LENAKER, P. A., ASKIN, R. A., MILLER, M. F. and BABCOCK, I. E., 2003. Reevaluation of the timing and extent of late Paleozoic glaciation in Gondwana: Role of the Transantarctic Mountains*, Geology,* 31:, 977–980.

JENNY–DESHUSSES, C., 1983. "Le Permian de l´Elborz Central et Oriental (Iran): Stratigraphie et micropaleontologie (Foraminifères et Algues)." Unpubl. These, no. 2130, University de Genev, Section des sciences de la terre, Geneva, 265 pp.

JOHNSON, B., 1981. Microfaunal biostratigraphy of the Dalan Formation (Permian) Zagros Basin, southwestern Iran. In: Neale, J. W. and Brasier, M. D., Eds., *Microfossils from recent and fossil shelf seas*, 52–61. London: British Micropaleontologival Society.

KAHLER, F., 1974. Iranische Fusuliniden. *Jahrbuch der Geologie, Abt B. –A.,* 117: 75–107.

———, 1977. Fusuliniden aus der Mediterranische-Iranische Gebiet. *Neues Jahrbuch fûr Geologie und Paleontologie,* 4: 199–216.

KAHLER. F./ and KAHLER, G., 1980. Fusuliniden (foraminifers) aus dem Karbon und Perm von Westanatolien und dem Iran. *Mitteilungen der Österreichischen Geologischen Gesellschaft*, 70: 187–269.

LASEMI, Y., 2001. *Facies analysis, depositional environments and sequence stratigraphy of the upper Precambrian and Paleozoic rocks of Iran*. Tehran: Geological Survey of Iran, 180 pp. (in Farsi).

LASEMI, Y., GHOMASHI, M., AMIN–RASOULI, H. and KHERADMAND, A., 2008. The lower Triassic Sorkh shale Formation of the Tabas block, east–central Iran: Succession of a failed basin at the Paleotethys margin, *Carbonates and Evaporites*, 23: 21–38.

LEVEN, E. Ja. and TAHERI, A., 2003. Carboniferous–Permian stratigraphy and fusulinids of East Iran. Gzhelian and Asselian deposits of the Ozbak–Kuh region. *Rivista Italiana di Paleontologia e Stratigrafia* ,109: 21–38.

LEVEN, E. Ja. and VAZIRI MOGHADDAM, H., 2004. Carboniferous–Permian stratigraphy and fusulinids of eastern Iran, The Permian in the Bagh–e– Vang section (Shirgesht area). *Rivista Italiana di Paleontologia e Stratigrafia*, 110:, 441–465.

LONGMAN, M. W., 1981. A process approach to recognizing facies of reef complexes. In: D. F. Toomey, Ed., *European Fossil Reef Models*, 9-40. Tulsa: SEPM (Society for Sedimentary Geology). Special Publication 30,

LUBESEDER, S., REDFERN, J. and BOUTIB, L., 2009. Mixed siliciclastic–carbonate shelf sedimentation–Lower Devonian sequences of the SW Anti–Atlas, Morocco. *Sedimentary Geology*, 215: 13–32.

MACK, G. H. and JAMES, W. C., 1985. Cyclic sedimentation in the mixed siliciclastic–carbonate Abo–Hueco transitional zone (Lower Permian), Sothwestern New Mexico. *Journal of Sedimentary Petrology,* 56: 635–647.

MAZULLO, S. J., 1992. Geochemical and neomorphic alternation of dolomite. A review. *Carbonates and Evaporites*, 7: 21–37.

MYROW, P. M. and LANDING, E., 1992. Mixed siliciclastic–carbonate deposition in an early Cambrian oxygen–stratified basin. Chapel Island Formation. Southeast Newfoundland: *Journal of Sedimentary Petrology,* 62: 455–473.

NICHOLS, G., 2000. Sedimentology and Stratigraphy. Oxford, Blackwell Science, 355 pp.

NOGOLE SADAT, M. A., 1978. "Les zones de decrochement et les virgations structurales en Iran. Consequences des resultants de l'analyse structurales de la region de Qom." Unpubl. Ph. D. Thesis, University Scientifique et Medicate de Gernoble, 201 pp.

PARTOAZAR, H., 1992. Changsingian stage in east Iran. Discovery of genus Colaniella and its biostratigraphic importance. *Geological Survey of Iran Geosciences Periodical,* 3: 44–53 (in Farsi with English abstract).

READ, J. F., 1982. Carbonate platforms of passive (extensional) continental margins: types, characteristics and evolution. *Tectonophysics,* 81: 195–212.

———, 1985. Carbonate platform facies models. *American Association of petroleum Geologists Bulletin,* 69: 1–12.

READ, J. F., OSLEGER, D. and ELRICK, M., 1991. Two–dimensional modeling of carbonate ramp sequences and component cycles. In: Franseen, E. K., Watney, W. L,, Kendall, C. G. St. C. and Rose, S, W., Eds., *Sedimentary modeling:computer simulations and methods for improved parameter definition,* 473–488. Lawrence: Kansas Geological Survey. Bulletin 233.

READING, H. G., 1996. *Sedimentary environments: processes, facies and stratigraphy.* Oxford: , Blackwell Science, 688 pp.

ROSS, R. P. and ROSS, C. A., 2003. Permian sequence stratigraphy and fossil zonation. In: Embry, A.F., Beauchamp, B., and Glass, D.J., Eds., *Pangea: Global environment and resources,* 219–231. Calgary: Canadian Society of Petroleum Geologists. Memoir 17.

RUTTNER, A., NABAVI, M. and HAJIAN, J., 1968. *Geology of the Shirgesht area (Tabas area, East Iran).* Tehran: Geological Survey of Iran. Report 4, 133 pp.

SCOTESE, C. R. and LANGFORD, R. P., 1995. Pangea and the paleogeography of the Permian. In: Scholl, P. A, Peryt, T. M. and Ulmer-–Scholl, D. S., Eds., *The Permian of Northern Pangea*, *Part I,* 3–19. Berlin: Springer–Verlag,

SENGOR, A. C., 1984. *The Cimmeride orogenic system and the tectonics of Eurasia.* Boulder: Geological Sciety of America. Special Paper, 195, 82 pp.

SHARLAND, P. R., ARCHER, R., CASEY, D. M., DAVIES, R. B., Hall, S. H., HEWARD, A. P., HORBURY, A. D. and SIMMONS, M. D., 2001. *Arabian plate sequence stratigraphy.* Bahrein: GeoArabia Special Publication 2, 371 pp.

SHINN, E. A., 1983. Tidal flat environment. In: Scholl, P. A., Bebout, D. G. and Moore, C. H., Eds., *Carbonate depositional environment,* 173–210.. Tulsa: American Association of Petroleum Geologists. Memoor 33

———, 1986. Modern carbonate tidal flats: their diagnostic features. *Quarterly Journal of Colorado School of mines,* 81: 7–35.

SIBLEY, D. F. and GREGG, J. M., 1987. Classification of dolomite rock texture. *Journal of Sedimentary Petrology*, 57: 697–975.

STOCKLIN, J., EFTEKHARNEJAD J. and HUSHMANDZADEH, A., 1965. *Geology of the Shotori Range (Tabas area, East Iran),* Tehran: Geological Survey of Iran, Report 3, 69 pp.

———, 1971. *Stratigraphic Lexicon of Iran. Part I, Central, North and East Iran,* Tehran: Geological Survey of Iran, Report 18, 338 pp.

———, 1977. Structural correlation of the Alpine ranges between Iran and Central Asia. *Memoires hors-series de la Societé géologique de France*, 8: 333–353.

SZABO, F. and KHARADPIR, A., 1978. Permian and Triassic stratigraphy, Zagros Basin, South–West Iran. *Journal of Petroleum Geology*, 1: 57–82.

TAKIN, M., 1972. Iranian geology and continental drift in the Middle East. *Nature*, 235: 147–150.

TUCKER, M. E. and WRIGHT, V. P., 1990. *Carbonate sedimentology.* London: Blackwell. 482 pp.

TUCKER, M. E., CALVET, F. and HUNT, D., 1993. Sequence stratigraphy of carbonate ramps: system tracts, models and application to the Muschelkalk carbonate platforms of eastern spain. In: Postamier, H. W., Summerhayes, C. P., Haq, B. U. and Allen, G. P., Eds., *Sequence stratigraphy and facies associations,* 397–415.*,* International Association of Sedimentologists, Special Publication, 18

WENDT, J., KAUFMANN, B., BELKA, Z., FARSAN, N. and B AVAND PUR, A. K, 2002. Devonian/Lower Carbonifeous stratigraphy, facies patterns and palaeogeography of Iran, Part I, Southeastern Iran, *Acta Geologica Polonica,* 52, 129–168.

WENDT, J.,, KAUFMANN, B., BELKA, Z., FARSAN, N. and BAVANDPUR, A. K., 2005. Devonian/Lower Carbonifeous stratigraphy, facies patterns and palaeogeography of Iran, Part II, Northern and Central Iran, *Acta Geologica Polonica,,* 55: 31–97.

WILSON, J. L., 1975. *Carbonate facies in geologic history.* Berlin, Springer–Verlag, 471 pp.

WRIGHT, V. P., 1986. Facies sequences on a carbonate ramp: the Carboniferous Limestone of South Wales. *Sedimentology,* 33: 221–241.

Received
Accepted
Published